Canadian Journal of
Earth Sciences

Article

Age and significance of the Fire Bay assemblage: an Ordovician arc fragment within the Clements Markham belt, northwestern Ellesmere Island, Canada

Megan M. Koch[a], **Karol Faehnrich**[b], **William C. McClelland**[a], **James L. Crowley**[c], **Michael J. Melchin**[d], **Luke P. Beranek**[e], **and Justin V. Strauss**[b]

[a]Department of Earth and Environmental Sciences, University of Iowa, 115 Trowbridge Hall, Iowa City, Iowa 52242, USA; [b]Department of Earth Sciences, Dartmouth College, HB6105 Fairchild Hall, Hanover, NH 03755, USA; [c]Department of Geosciences, Boise State University, 1910 University Dr., Boise, Idaho 83725, USA; [d]Department of Earth Sciences, St. Francis Xavier University, Antigonish, NS B2G 2W5, Canada; [e]Department of Earth Sciences, Memorial University of Newfoundland, 9 Arctic Avenue, St. John's, NL A1B 3X5, Canada

Corresponding author: **William C. McClelland** (email: bill-mcclelland@uiowa.edu)

Abstract

The Fire Bay Formation of Trettin (1998), Clements Markham belt, Ellesmere Island, Canada, includes volcanic rocks described as Silurian in age based on Llandovery graptolites in adjacent clastic rocks. New field observations suggest the Llandovery fossils are from packages of the Silurian Danish River and/or Lands Lokk formations that are fault-bounded rather than stratigraphically tied to Ordovician sections that contain a 470.0 ± 0.2 Ma lithic tuff, volcaniclastic units with maximum depositional ages (MDAs) of 466 ± 2 and 462 ± 2 Ma based on detrital zircon, volcanic clasts with ages of 498 ± 6, 478 ± 4, and 477 ± 8 Ma, and Ordovician conodonts and graptolites of Darriwilian and Sandbian age, respectively. Since the Fire Bay Formation of Trettin (1998) lacks a type section and is fault-bounded with ambiguous age relationships, Ordovician volcanic units and fault-bounded clastic rocks correlated with the Hazen Formation are both included in the Fire Bay assemblage following the original interpretations of Trettin and Nowlan (1990). The Fire Bay assemblage records juvenile Ordovician arc magmatism proximal to the Pearya terrane. The adjacent Lands Lokk Formation yields bimodal age peaks at 440–430 and 465 Ma, MDA of 424 ± 3 Ma, and $\varepsilon Hf_{(t)}$ values of −5 to +10. The signature matches Ordovician Pearya units and Silurian circum-Arctic arc sources but there is no evidence for Silurian arc magmatism between the Pearya terrane and Laurentian margin, compatible with Pearya accretion during oblique Ordovician arc collision and Silurian sinistral translation along the northern Laurentian margin.

Key words: U/Pb dating, Pearya terrane accretion, Ordovician arcs, biostratigraphy, detrital zircon, Ellesmere Island

Résumé

La Formation de Fire Bay deTrettin (1998), de la ceinture de Clements Markham de l'île d'Ellesmere (Canada), comprend des roches volcaniques décrites comme étant d'âge silurien à la lumière de graptolites llandovériens dans des roches clastiques attenantes. De nouvelles observations de terrain portent à croire que les fossiles llandovériens proviennent de paquets des formations siluriennes de Danish River ou de Lands Lokk qui sont bordés par des failles plutôt que d'être reliés stratigraphiquement à des séquences ordoviciennes qui contiennent un tuf lithique de 470,0 ± 0,2 Ma, des unités volcanoclastiques d'âge de dépôt maximum (ADM) de 466 ± 2 Ma et 462 ± 2 Ma à la lumière de zircons détritiques, des clastes volcaniques ayant produit des âges de 498 ± 6 Ma, 478 ± 4 Ma et 477 ± 8 Ma et des conodontes et graptolites ordoviciens d'âge darriwillien et sandbien, respectivement. Comme la Formation de Fire Bay de Trettin (1998) n'a pas de coupe type et est bordée par des failles dont les relations d'âge sont ambiguës, des unités volcaniques ordoviciennes et des roches clastiques bordées par des failles corrélées à la Formation de Hazen sont incluses dans l'assemblage de Fire Bay, suivant les interprétations initiales de Trettin et Nowlan (1990). L'assemblage de Fire Bay témoigne d'un magmatisme d'arc ordovicien proximal par rapport au terrane de Pearya. La Formation de Lands Lokk attenante donne des pics d'âges bimodaux à 440–430 Ma et 465 Ma, un ADM de 424 ± 3 Ma et des valeurs de $\varepsilon Hf_{(t)}$ de −5 à +10. Cette signature concorde avec des unités ordoviciennes de Pearya et des sources d'arc circumarctique siluriennes, mais il n'y a aucun indice de magmatisme d'arc silurien entre le terrane de Pearya

et la marge laurentienne, ce qui est compatible avec l'accrétion de Pearya durant la collision oblique d'un arc ordovicien et une translation senestre silurienne le long de la marge septentrionale de la Laurentie. [Traduit par la Rédaction]

Mots-clés : datation U/Pb, accrétion du terrane de Pearya, arcs ordoviciens, biostratigarphie, zircon détritique, île d'Ellesmere

Introduction

The Pearya terrane on the northern margin of Laurentia plays a critical role in tectonic models for the Paleozoic evolution of the circum-Arctic region that advocates for large-scale transfer of terranes from the Caledonian and Timanian orogens in the east to the Cordilleran orogen on the west (McClelland et al. 2022 and references therein). The "Northwest Passage" model of Colpron and Nelson (2009) assumes an exotic origin for the Pearya terrane, which is located outboard of deep-water passive margin deposits of the Franklinian Basin on northern Ellesmere Island, Nunavut, Canada (Fig. 1; Churkin and Trexler 1980; Trettin 1987). The Pearya basement is predominantly Tonian orthogneiss structurally overlain by Neoproterozoic to early Paleozoic metaclastic and metavolcanic rocks (Trettin 1998). Juxtaposition of these basement units with Early Ordovician mafic and ultramafic rocks during the M'Clintock orogeny (Trettin 1987; Estrada et al. 2018; Majka et al. 2021) was accompanied by Ordovician arc-related magmatism (Malone et al. 2019).

An arc origin for Ordovician magmatic rocks of the Pearya terrane is consistent with models invoking migration of Paleozoic arc fragments of varied origins along the northern Laurentian margin (Strauss et al. 2013; Beranek et al. 2013*a*, 2013*b*, 2015; White et al. 2016; Pecha et al. 2016). However, allochthoneity of the Pearya terrane and the timing and nature of its accretion to the northern Laurentian margin remain uncertain. Models for the history of Pearya include accretion of a composite arc fragment along the Franklinian margin by arc–continent collision (Klaper 1992; Bjørnerud and Bradley 1992; Trettin 1998; Dumoulin et al. 2000) or displacement on a transpressional sinistral strike–slip system (Trettin 1998; Malone et al. 2017, 2019; Estrada et al. 2018; McClelland et al. 2021). Alternative models suggest minimal displacement of a parautochthonous pericratonic fragment on the rifted Franklinian margin (Hadlari et al. 2014; Dewing et al. 2019). The accretion models require a transform or subduction boundary between the Pearya terrane and Laurentian margin with hybrid models for oblique convergence permissible, whereas minimal displacement models assume the Pearya terrane is the undisrupted continuation of the Laurentian margin.

The Pearya terrane is bound to the south by a complexly deformed package of Cambrian–Silurian sedimentary and volcanic units originally referred to as the Clements Markham fold belt (Trettin 1987) but herein referred to simply as the Clements Markham belt since the assemblage is defined by age and lithology rather than well-documented structural characteristics. The belt is divided into Successions A and B within geographically defined outcrop belts that are inferred to be distal equivalents of the Laurentian passive margin (Trettin 1998). Succession A includes Cambrian–Ordovician deep-marine sedimentary and volcanic rocks, as well as Silurian volcaniclastic units of the Fire Bay Formation (Trettin 1998). Succession B is a generally shallowing-upward sequence of deep-marine, synorogenic clastic rocks overlain by shallow-marine clastic and carbonate units that include the Silurian Danish River and Lands Lokk formations. The Danish River Formation is commonly designated as an overlap assemblage that marks juxtaposition of the Pearya terrane with the Laurentian margin (e.g., Trettin 1998). Final accretion of the Pearya terrane to the Laurentian margin occurred in the late Silurian to early Late Devonian (Malone et al. 2019) followed by post-accretionary translation along the margin (McClelland et al. 2021).

In this context, the age and tectonic setting of Ordovician and Silurian igneous rocks within the Clements Markham belt are critical to understanding the mechanism of Pearya emplacement on the Laurentian margin. For example, Ordovician arc rocks have long been cited as evidence for closure of a major ocean basin between Pearya and Laurentia (Trettin 1987, 1998; Bjørnerud and Bradley 1992; Klaper 1992); however, the presence of Silurian arc-related volcanic rocks in the Fire Bay Formation of Trettin (1998) that are in part coeval with Silurian syn-orogenic turbidites in the Clements Markham belt has been used to suggest ocean basin closure was not complete until Silurian time (Beranek et al. 2015). Trettin (1998) defined the Fire Bay Formation as a succession of Silurian (Llandovery) interlayered volcanic and sedimentary rocks based on a composite of measured stratigraphic sections tied to several key graptolite localities near Fire Bay of Emma Fiord, northwestern Ellesmere Island (Fig. 1). Beranek et al. (2015) confirmed this Silurian age assignment through detrital zircon U/Pb analysis of archived samples collected during the original field work of Hans Trettin and the Geological Survey of Canada (GSC). Additional samples for geochronologic, geochemical, and paleontological analyses were collected during a 2017 field program designed to re-examine the structural and stratigraphic field relationships of Ordovician and Silurian volcanic and sedimentary rocks in the Fire Bay region (Fig. 2). The results presented below indicate that the original Fire Bay Formation of Trettin (1998) includes a variety of different fault-bounded rocks. On this basis, we propose revisions to the stratigraphic architecture of this unit (Fig. 3) and place it within the regional tectonic framework for the Clements Markham belt.

Early Paleozoic geology of the Fire Bay area

The remarkable reconnaissance work of Hans Trettin and colleagues at the GSC provides the current stratigraphic framework for our understanding of the pre-Carboniferous geology of northern Ellesmere Island (e.g., Trettin 1998). Early Paleozoic rocks of the Emma Fiord region were originally assigned to the lower Silurian (Llandovery) Imina and Lands Lokk formations (Trettin 1969), the latter of which was subdivided into three members (A–C). Member B of the Lands Lokk Formation, recognized only in the Fire Bay area and a small area east of Emma Fiord (Trettin 1969) comprised undated volcanic conglomerate, mudstone, tuff, and minor limestone.

Fig. 1. Generalized map showing the major structural and lithologic units in the Franklinian basin and Pearya terrane of northern Ellesmere Island and the location of the Fire Bay area. The figure location is shown in the inset. Major faults include the Pearya shear zone (PSZ), the Emma Fiord (EF), Inlet Head (IH), Petersen Bay (PB), and Lake Hazen (LH) fault zones, and the Porter Bay (PoB), M'Clintock Glacier (MG), and Mount Rawlinson (MR) faults. Map is modified from Trettin (1998) and Piepjohn et al. (2016). [Colour online.]

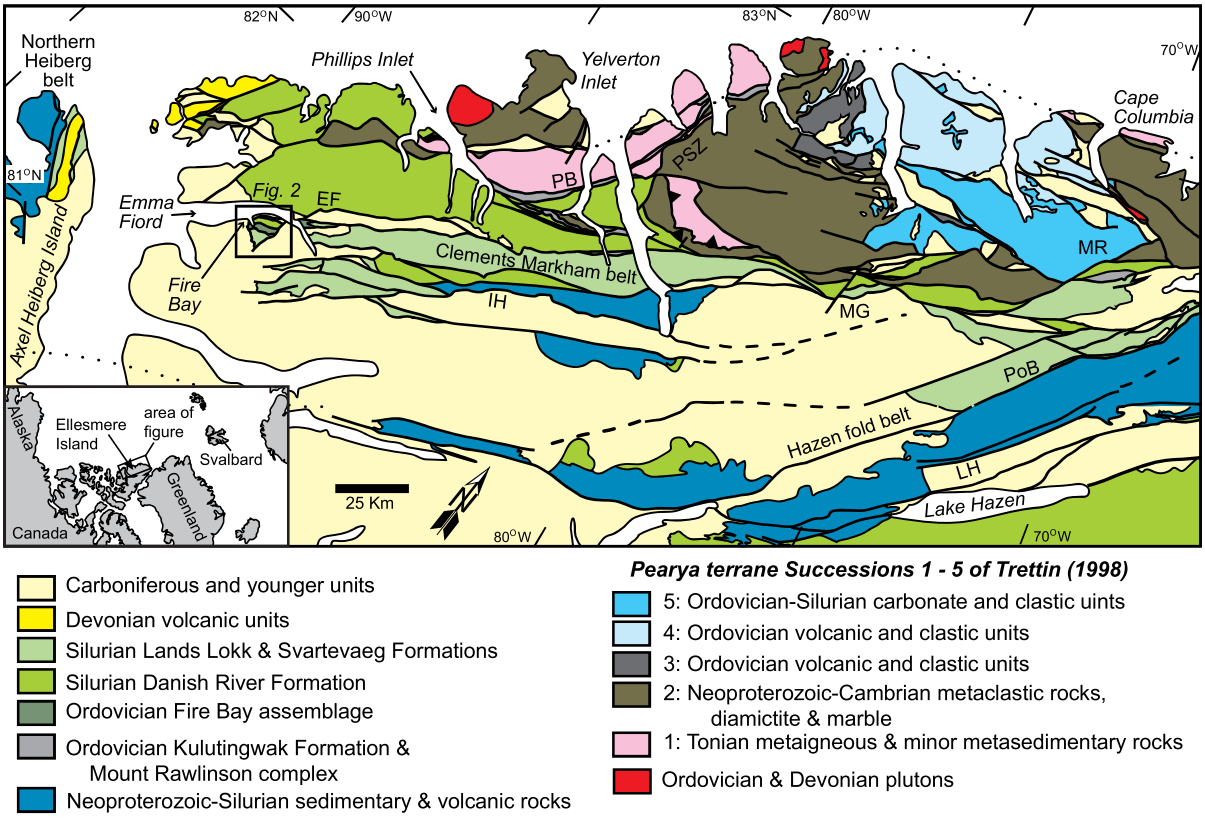

These strata were considered Llandovery in age based on their assumed stratigraphic position between graptolite-bearing strata of Members A and C; however, the subsequent recognition of Middle Ordovician (now Early–Middle or Floian–Darriwilian) conodonts in carbonate olistoliths of Member B led Trettin and Nowlan (1990) to reassign these strata to the informal Middle Ordovician Fire Bay assemblage. This assemblage included (1) a recessive suite of dark grey slate, chert, and minor tuff with carbonate lenses and olistoliths and (2) a resistant package of volcanic rocks with rare carbonate lenses. Both units of the Middle Ordovician Fire Bay assemblage were assumed to be in fault contact with the lower Silurian Lands Lokk Formation (Trettin and Nowlan 1990).

In his later synthesis of the regional geology of northern Ellesmere and Axel Heiberg Islands, Trettin (1998) abandoned both of these previous nomenclatural schemes and instead subdivided rocks surrounding Fire Bay into the Hazen, Fire Bay, and Danish River formations (Fig. 3). More specifically, he assigned the recessive suite of Lower–Upper Ordovician (Floian–Sandbian; age updated in Trettin 1998) interbedded dark grey chert, slate, and carbonate to the Hazen Formation based on correlations with similar aged strata in the Hazen fold belt (Fig. 1; Trettin 1994), and he combined the resistant package of volcanic rocks and minor carbonate of the Fire Bay assemblage with lower Silurian (Llandovery) clastic rocks of Member A of the Lands Lokk Formation to formalize the Fire Bay Formation. A thin belt of lower–middle Silurian (Llandovery?) strata northwest of the newly defined Fire Bay Formation, which was previously mapped as part of Member B of the Lands Lokk Formation (Trettin 1969) was separated out as the Danish River Formation (Trettin 1994) based on correlations with Silurian–Devonian clastic rocks in the Hazen fold belt (Fig. 1; Trettin 1998).

The ~500–600 m thick Fire Bay Formation was subdivided by Trettin (1998) into three members (A–C; Fig. 3), and Member A was further distinguished across two local facies belts in Fire Bay (referred to as the northwestern and southeastern facies of Member A). Member A was subdivided into four informal units of predominantly fine-grained clastic rocks with minor coarse-grained serpentinite- and chromite-bearing volcaniclastic strata and rare carbonate olistoliths, Member B was subdivided into two informal units comprised largely of volcanic rocks with rare carbonate olistoliths, and Member C was differentiated as a poorly exposed graptolitic mudstone unit (Trettin 1998). The early Silurian age of the Fire Bay Formation was assigned based on an isolated outcrop of early late Llandovery graptolitic mudstone in Member A (F12 in Fig. 2) and a single collection of middle to late Llandovery (Aeronian or Telychian) graptolites obtained from Member C (F13 in Fig. 2; Trettin 1998). As outlined below, new field

Fig. 2. Simplified geologic map of the Fire Bay area, northeastern Ellesmere Island, Canada, showing the location of samples discussed in this study. Map is modified from Trettin (1996) and Harrison et al. (2015) based on field observations made during this study. Fossil localities F1–F15 are from Trettin (1998). Detrital zircon sample locations C-242700, C-242744, and C-242858 are from Beranek et al. (2015). Abbreviation: Fm, formation. Map projection is in WGS84. [Colour online.]

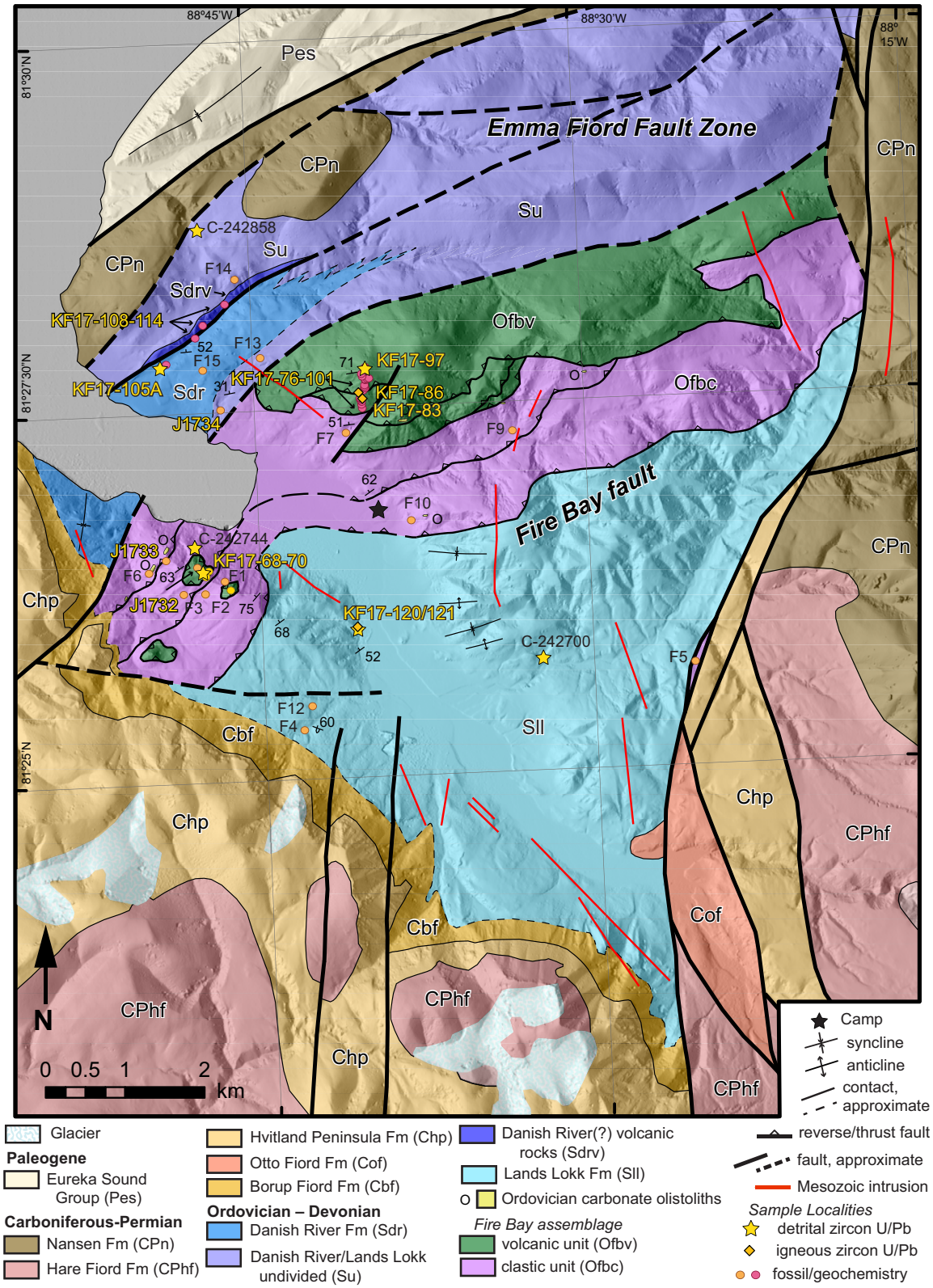

observations and geochronologic data suggest that the fossiliferous Silurian strata are structurally separated from Ordovician units such that depositional relationships inferred for the composite Fire Bay Formation of Trettin (1998) and correlation of Ordovician units with the Hazen Formation across several major faults to the south are unlikely.

Methods

Fieldwork

Outcrops in the Fire Bay area were examined and sampled during a 5-day campaign in August 2017. Stratigraphic sections previously described by Trettin (1998) were accessed by foot traverses from a central camp at the head of Fire Bay (black star in Fig. 2). Field observations provide the stratigraphic and structural framework for a modified reconnaissance geologic map of the Fire Bay area (Fig. 2), as well as the sampling framework for geochronologic, geochemical, and biostratigraphic samples (Supplementary Data S1).

Geochronology and geochemistry

Nine samples were collected for zircon U/Pb geochronology from the Fire Bay, Danish River, and Lands Lokk formations of the Clements Markham belt. The sample locations are shown on Figs. 2–4 and listed in Supplementary Data S1. Heavy mineral separates were retrieved from each sample by standard crushing, density and magnetic separation techniques at the University of Iowa and Dartmouth College. Zircon from six of the igneous and detrital zircon samples were analyzed by laser ablation-inductively coupled mass spectrometry (LA–ICP–MS) for U/Pb and Hf isotopes at the Arizona LaserChron Center and U/Pb isotopes and trace elements at Boise State University. Secondary ion mass spectrometry (SIMS) U/Pb samples previously reported by Beranek et al. (2015) were also measured for Hf isotopes by ICP–MS at Washington State University. Three igneous and detrital zircon samples were analyzed for U–Th–Pb isotopes and trace elements by SIMS at the Stanford-US Geological Survey Micro-Analysis Center. Finally, single zircon grains from sample KF17-83 in the Fire Bay Formation of Trettin (1998) were plucked from an epoxy mount after LA–ICP–MS analysis and analyzed by the chemical abrasion-isotope dilution-thermal ionization mass spectrometry (CA–TIMS) method (Mattinson 2005) at Boise State University. The analytical methods are all described in detail in Supplementary Data S2 and the complete data sets are presented in Supplementary Data S3–S5. Representative cathodoluminescence (CL) images of zircon grains for each sample are presented in Supplementary Data S6.

The U/Pb data obtained from each sample are treated according to the interpreted protolith. Dates obtained from igneous protoliths are pooled together to obtain weighted mean $^{206}Pb/^{238}U$ ages or Concordia ages using Ludwig (2008) and reported at the 95% confidence level. The filtering criteria and methods for handling detrital zircon are described in Supplementary Data S2. Estimates of the maximum depositional age (MDA) are interpreted in the context of maximum likelihood age (MLA) estimates (Vermeesch 2021) and

Fig. 3. Simplified stratigraphic column for exposures of early Paleozoic rocks in the Fire Bay area, Ellesmere Island, modified after Trettin (1998). Note the stratigraphic location of samples described in the main text and displayed on the geologic map (Fig. 2), as well as the differences in nomenclature between Trettin (1998) and our study. The exact sample locations of Beranek et al. (2015) are schematic since they were retrieved from Geological Survey of Canada (GSC) archives. Abbreviations: A, assemblage; DR, Danish River; Fm, formation; fms, formations; LL, Lands Lokk; Mb, member. [Colour online.]

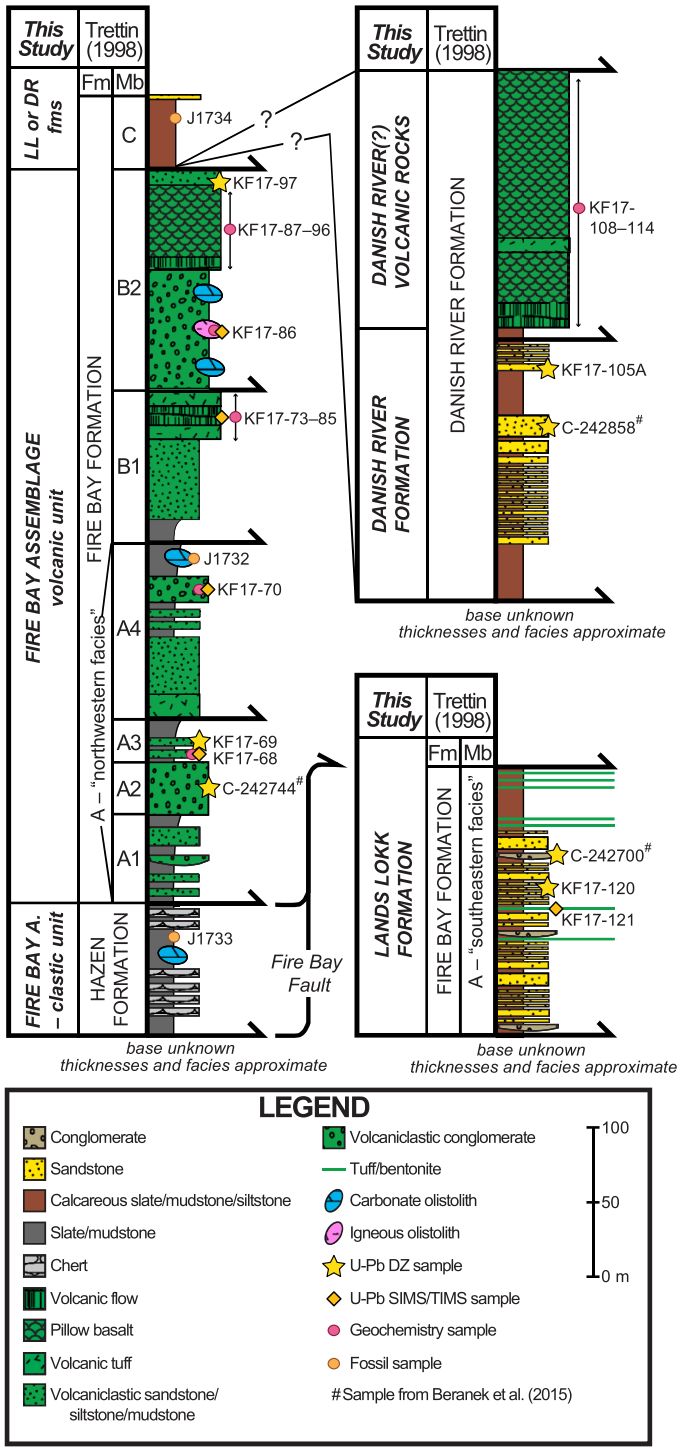

Fig. 4. Photographs of the Fire Bay area showing relationships discussed in the text. (*a*) Looking NW at outcrop exposures around the Emma Fiord Fault Zone of the northern Fire Bay area that are characterized by widespread cover by Quaternary glacial debris. The prominent drainage has the best exposures of the Danish River Formation and Danish River(?) volcanic rocks. (*b*) Subvertical lithic arenite beds of the Danish River Formation; geologists for scale. These beds were sampled for detrital zircon U/Pb geochronology (sample KF17-105A). (*c*) Loading structures and flutes on the sole of a lithic arenite bed in the Danish River Formation; hammer is 33 cm long. (*d*) Steeply dipping exposure of pillow basalts and minor flows and breccias of the Danish River(?) volcanic rocks; geologist circled for scale. (*e*) Exposure of pillow basalts in the Danish River(?) volcanic rocks; hammer is 33 cm long. (*f*) Tectonized subvertical contact (yellow dashed line) of interbedded lithic arenite and mudstone of the Danish River Formation with pillow basalts of the Danish River(?) volcanic rocks; circled hammer is 33 cm long. (*g*) Close-up of silicified zone at contact between Danish River lithic arenite bed and amygdaloidal pillow basalt of the Danish River(?) volcanic rocks; pencil is 14.2 cm long. (*h*) Steeply dipping beds of the Lands Lokk or Danish River formations at fossil locality J1734 (see Fig. 2); geologist circled for scale. These strata were originally mapped as Member C of the Fire Bay Formation by Trettin (1998). [Colour online.]

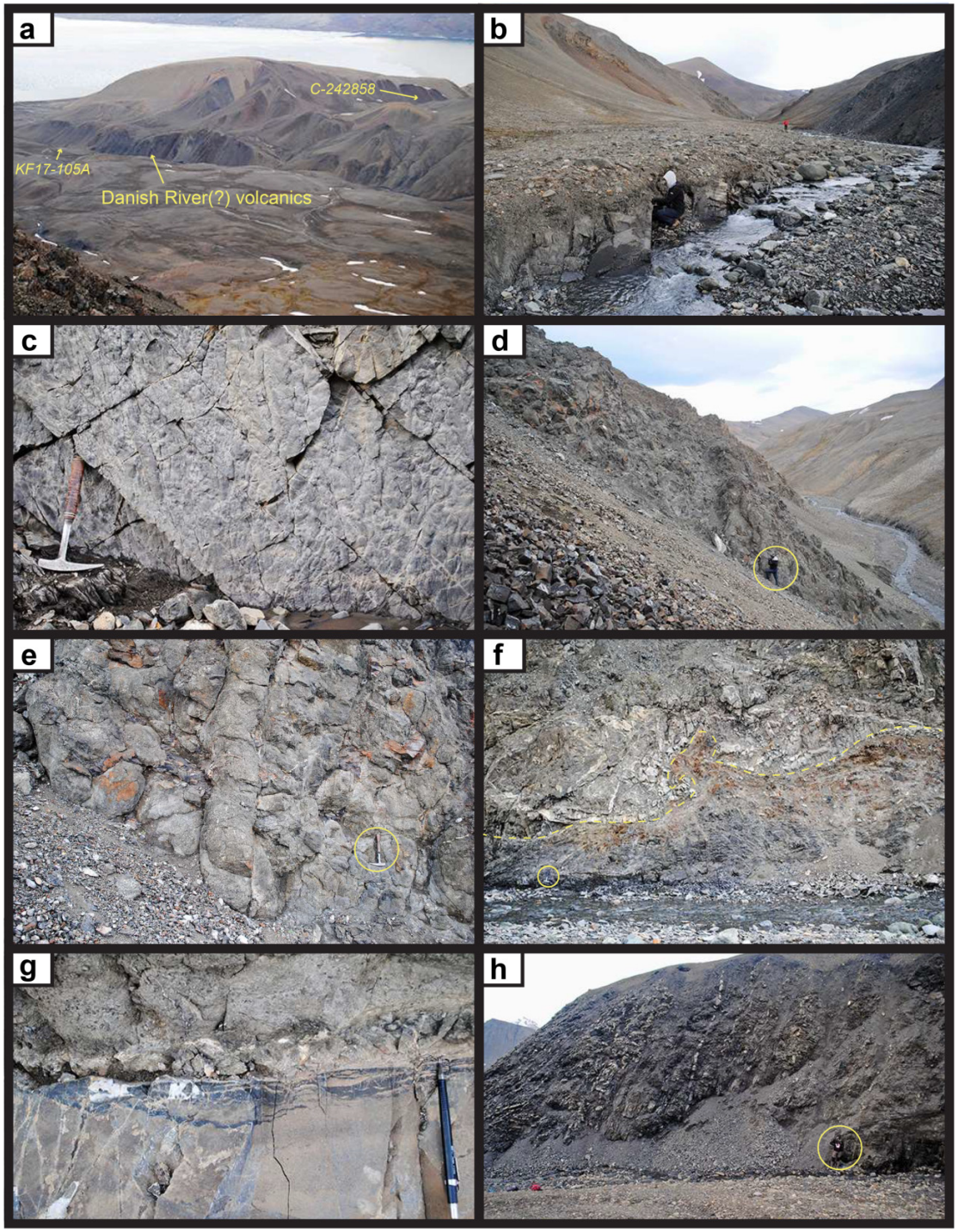

youngest age populations from the TuffZirc and Unmix methods (Ludwig 2008). Quantitative comparison of samples in this study and with other regional data sets is based on Kolmogorov–Smirnov D values (Vermeesch 2018*a*; Saylor and Sundell 2016) and presented as three-dimensional multidimensional scaling plots using the DZmds routine of Saylor et al. (2017).

Twenty-two igneous samples were collected for whole-rock geochemistry from the following units: (1) mafic to felsic flows and pillow basalts of the Fire Bay Formation, (2) felsic igneous clasts from volcaniclastic conglomerates of the Fire Bay Formation, and (3) mafic dikes and flows associated with the Danish River Formation (Fig. 2). The sample locations and analytical methods are provided in Supplementary Data S1 and S2. Four of these samples were analyzed for Nd and Sr isotope geochemistry, the detailed methods of which are explained in Supplementary Data S2. The whole-rock geochemical and isotopic data sets are presented in Supplementary Data S7 and S8.

Results

Field observations, biostratigraphic data, and proposed nomenclature

As highlighted above, Trettin (1998) redefined the stratigraphic architecture for early Paleozoic exposures around Fire Bay after multiple iterations of reconnaissance mapping in the Emma Fiord region (e.g., Trettin 1969, 1996; Trettin and Nowlan 1990; Trettin and Mayr 1996). Building upon Trettin's work, we use new detailed field observations and analytical data to re-evaluate the regional stratigraphy around Fire Bay to reflect that most of the major map units are fault-bounded and have conflicting and/or ambiguous age relationships (Figs. 2 and 3). Specifically, we propose abandoning the formalization of the Fire Bay Formation of Trettin (1998) for the following reasons: (1) the lack of a continuous type section, (2) the exposure of this unit in fault-bounded slivers with no coherent stratigraphic architecture beyond single outcrops that were used to define its members, and (3) ambiguity in its age relationships with adjacent map units. Similarly, we suggest abandoning the use of Hazen Formation in the Fire Bay region because this unit (1) lacks a reference section, (2) is exposed in fault-bounded slivers with no coherent stratigraphic architecture, and (3) is separated by hundreds of kilometres across several major structural boundaries from the type area of the Hazen Formation in the Hazen fold belt (Fig. 1; Trettin 1994). Instead, we suggest reverting to Trettin and Nowlan's (1990) definition of the informal Fire Bay assemblage (Fig. 3), which is characterized by two informal units, one dominated by volcanic rocks (Fire Bay Formation of Trettin 1998) and another dominated by clastic rocks (Hazen Formation of Trettin 1998). For historical purposes and to make our proposed changes abundantly clear, below we include Trettin's (1998) unit designations in our descriptions of field observations and sample locations. Despite these contrasts in our stratigraphic interpretations, Trettin (1998) provided a very thorough and accurate review of the early Paleozoic lithofacies. Below, we build upon these detailed descriptions by focusing on where our own observations provide new data and/or interpretations to support our revised regional stratigraphic assignments.

The Fire Bay assemblage is exposed along the southern edge of the ~0.2–5 km wide, >150 km long Emma Fiord Fault Zone (Figs. 1 and 2; Trettin 1996, 1998; Trettin and Mayr 1996), which is a major polyphase structural boundary within the Clements Markham belt that was most recently reactivated during the Eocene Eurekan orogeny (Trettin 1998; Piepjohn et al. 2013; Brandes and Piepjohn 2021). Deformation related to the Emma Fiord Fault Zone is exemplified by an anastomosing series of poorly exposed high-angle faults with undocumented kinematics that juxtapose multiple Paleozoic and younger units in Fire Bay (Fig. 2), as well as broad upright folding and local cleavage development in the Paleogene Eureka Sound Group. This deformation severely complicates evaluating primary stratigraphic relationships between early Paleozoic map units in the northern Fire Bay area, specifically between exposures of the Fire Bay assemblage and the Danish River and Lands Lokk formations (Fig. 2).

Most of the outcrops in the fault-bounded portion of the northern Fire Bay area are covered by glacial drift in low relief hills and strand flats (Fig. 4*a*), and exposures are limited to stream cuts and rare steep hillsides with frost-shattered rubble (Fig. 4*b*). We focused our efforts in this region on examining previous fossil and detrital zircon sample locations (sites F13–F15 and C-242858 in Fig. 2; Trettin 1998; Beranek et al. 2015), as well as the contact between Members B and C of the Fire Bay Formation of Trettin (1998) and the overlying Danish River Formation. The Danish River Formation locally consists of interbedded dark grey calcareous shale, siltstone, and lithic arenite. These strata are commonly subvertical to moderately north-dipping (Figs. 2 and 4*b*), display inclined to upright and largely symmetrical folds, and record multiple cleavages depending on their proximity to poorly exposed fault strands of the Emma Fiord Fault Zone. Lithic arenite units within the Danish River Formation are medium- to thick-bedded and massive to laminated with full to partial Bouma sequences and prominent flutes, grooves, and loading structures (Figs. 4*b* and 4*c*). Along a prominent NE-trending unnamed subvertical fault in the northern map area, coarse-grained clastic rocks of the Danish River Formation are locally in contact with an ~75–150 m thick mafic volcanic package that includes highly weathered pillow structures, agglomerate, and breccia that is herein referred to as the Danish River(?) volcanic rocks with (?) signifying the uncertain relationship between the volcanic rocks and clastic units of the Danish River Formation (Figs. 2 and 4*d*–4*g*). Although the boundary between these two units is structurally modified (Fig. 4*f*), centimetre-scale exposures of the contact display an abrupt and highly silicified zone that most likely reflects a primary unlithified sediment–volcanic flow relationship (Fig. 4*g*). Mafic dikes that are locally up to ~5 m thick cut the Danish River Formation and appear to feed these volcanic rocks, but the presence of widespread Mesozoic mafic dikes throughout the broader map area (Trettin 1996; Trettin and Mayr 1996; Harrison et al. 2015) suggests they may at least in part be younger.

Trettin (1998) described Middle–Upper Ordovician fossiliferous carbonate olistoliths (e.g., F15 in Fig. 2), Silurian graptolites (F14 in Fig. 2), and Upper Devonian felsic porphyry in the Danish River Formation from the northern region of Fire Bay. Our observations suggest these samples were collected from isolated outcrops and/or rubble with no clear stratigraphic or intrusive relationships with surrounding rocks of the Danish River Formation (Fig. 4*a*). Similarly, sample C-242858 of Beranek et al. (2015) was collected from an isolated outcrop of lithic arenite that is lithologically similar to the Danish River Formation, but its relationship to the more coherent packages of this unit is ambiguous.

The contact between Trettin's (1998) Member C of the Fire Bay Formation and the overlying Danish River Formation was mapped as depositional based on an inferred younger-over-older Silurian stratigraphic relationship. More specifically, Trettin (1998) described two fossil localities from the Danish River Formation in the Clements Markham belt, one from site F14 near Fire Bay (Fig. 2; Trettin 1996) that yielded undifferentiated Silurian graptolites and bivalves, and another ~30 km ENE of the head of Emma Fiord that yielded late Llandovery graptolites (Trettin 1969). Middle to late Llandovery (late Aeronian or Telychian) graptolites collected from talus at site F13 near Fire Bay (Fig. 2) were inferred to constrain the age of Member C of the Fire Bay Formation (Trettin 1998). We revisited this locality and made an additional brachiopod and graptolite collection from outcrops along strike in a prominent stream drainage (J1734; Figs. 2 and 4*h*); these collections yielded specimens of *Colonograptus ludensis* or *Neocolonograptus ultimus*, which are most likely late Wenlock or early Pridoli in age (Fig. 5, see Supplementary Data S9). In addition, brachiopods in the collection suggest a late Llandovery to Wenlock, possibly Ludlow age (J. Jin, personal communication, 2018), indicating that the late Wenlock graptolite age is more likely. These fossils are much *younger* than graptolite collections from the overlying Danish River Formation in the Clements Markham belt, and are instead more consistent with published graptolite collections from the Lands Lokk Formation (Trettin 1998). Critically, there are no exposed contacts between Trettin's (1998) Member B volcanic rocks of the Fire Bay Formation and overlying fossiliferous strata of Member C in the area in general (Fig. 2; Trettin 1996) and these units have different structural attitudes across the unexposed contact at this locality. Given these ambiguous field and age relationships, we suggest that Trettin's (1998) Member C clastic rocks of the Fire Bay Formation should instead be mapped as either a fault-bounded package of the Lands Lokk or Danish River formations (Figs. 2 and 3).

Paleogene deformation related to the Emma Fiord Fault Zone is less pronounced in the southern Fire Bay area (Fig. 2), but stratigraphic relationships within the early Paleozoic units remain complex. Trettin (1996, 1998) proposed a simplified stratigraphic architecture in which Ordovician chert and mudrock of the Hazen Formation are depositionally overlain by different facies belts of Members A and B of the Silurian Fire Bay Formation. We recognized no primary depositional contacts between these units, nor did we confirm a prominent facies change within Trettin's (1998) Fire Bay Formation (Fig. 3). Instead, the field relationships define (1) a northern belt dominated by ~25–400 m thick north-dipping imbricate stacks of semicoherent to locally incoherent packages of diverse volcanic, volcaniclastic, and sedimentary rocks separated by several well-defined and a multitude of smaller scale N-dipping thrust faults (Figs. 2–3 and 6*a*) and (2) a southern belt of more coherent siliciclastic-dominated strata with locally abundant volcanic tuff and tuffaceous mudstone (Figs. 2 and 3). These two different structural-stratigraphic packages are juxtaposed by a prominent series of N-dipping thrust faults that we collectively refer to herein as the Fire Bay fault,

Fig. 5. Camera lucida drawings of the most biostratigraphically useful graptolite taxa encountered in this study. (*a*) *Colonograptus ludensis* (Murchison, 1839) or *Neocolonograptus ultimus* Perner, 1899, from fossil collection J1734 indicating a likely late Homerian (Wenlock, *Colonograptus ludensis* zone) or possibly early Pridoli (*Neocolonograptus ultimus* zone) age. (*b*) *Climacograptus bicornis* (Hall 1847), from fossil collection J1733, indicating a late Sandbian (early Late Ordovician) age (*Climacograptus bicornis* zone = *Orthograptus calcaratus* zone). (*c*) *Orthograptus calcaratus* (Lapworth, 1876), from sample J1733 indicating a late Sandbian age (*Climacograptus bicornis* zone = *Orthograptus calcaratus* zone). Scale bars = 1 mm. See Supplementary Data S9 for discussion of the faunas.

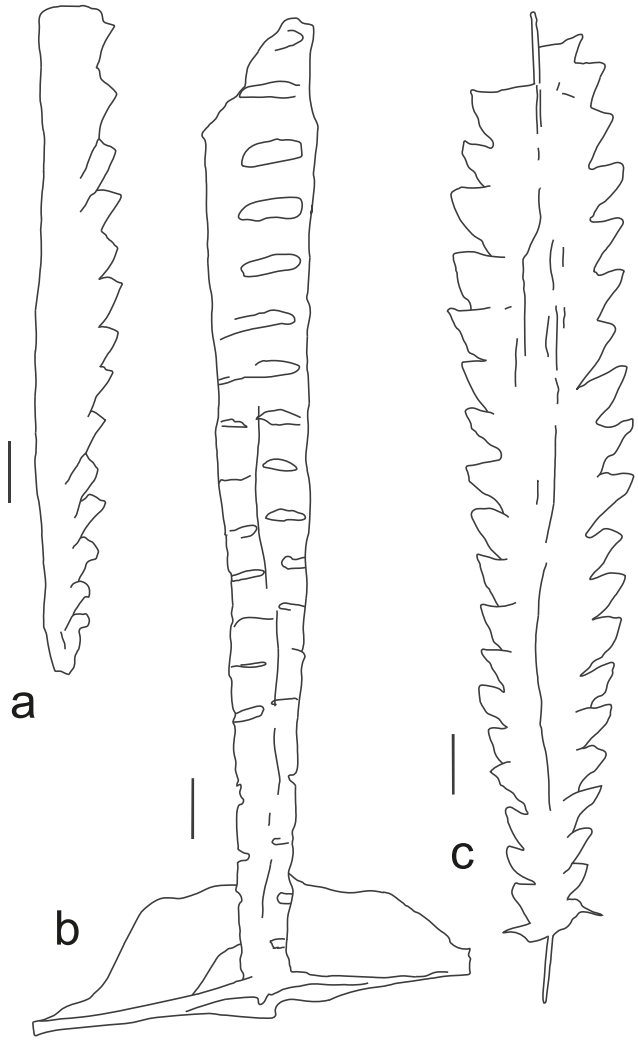

Fig. 6. Photographs of the Fire Bay area showing relationships discussed in the text. (*a*) Stitched panorama of the western side of Fire Bay showing the major geological relationships and key sample locations. The largest peak in the foreground is ~350 m tall, and the map unit abbreviations are the same as in Fig. 2. (*b*) Peaks on the eastern side of Fire Bay hosting the thickest exposure of Fire Bay assemblage volcanic/volcaniclastic rocks, as well as multiple decametre-scale olistoliths (vertical yellow arrows). Key volcanic and detrital zircon sample locations are shown on the ridge (also location of section 2 of Trettin 1998); tents are circled for scale. (*c*) Broken formation and olistostromal mélange exposed on the main peak shown in (*b*). Vertical yellow arrows denote location of decametre-scale olistoliths of igneous, volcanic, and carbonate rocks. (*d*) Polymict clast-supported boulder to cobble conglomerate at the top of Trettin's Member A4 of the Fire Bay Formation (Fire Bay assemblage of this contribution). A subrounded rhyolite clast in this horizon was sampled for U/Pb SIMS geochronology (KF17-70); hammer is 33 cm long. (*e*) Flow-banding preserved in lithic and crystal tuff from Member B1 in Trettin's (1998) section 2. This horizon was sampled for U/Pb CA–TIMS geochronology (KF17-83) and its location is shown in (*b*); coin is 1.9 cm in diameter. (*f*) Interbedded calcareous mudstone, lithic arenite, lithic wacke, and tuffaceous mudstone sampled for U/Pb geochronology in the Lands Lokk Formation (previously mapped as the southeastern facies of Member A of the Fire Bay Formation sensu Trettin 1998). (*g*) Close-up of graded calcareous lithic arenite bed in the Lands Lokk Formation displaying discrete Bouma subdivisions. [Colour online.]

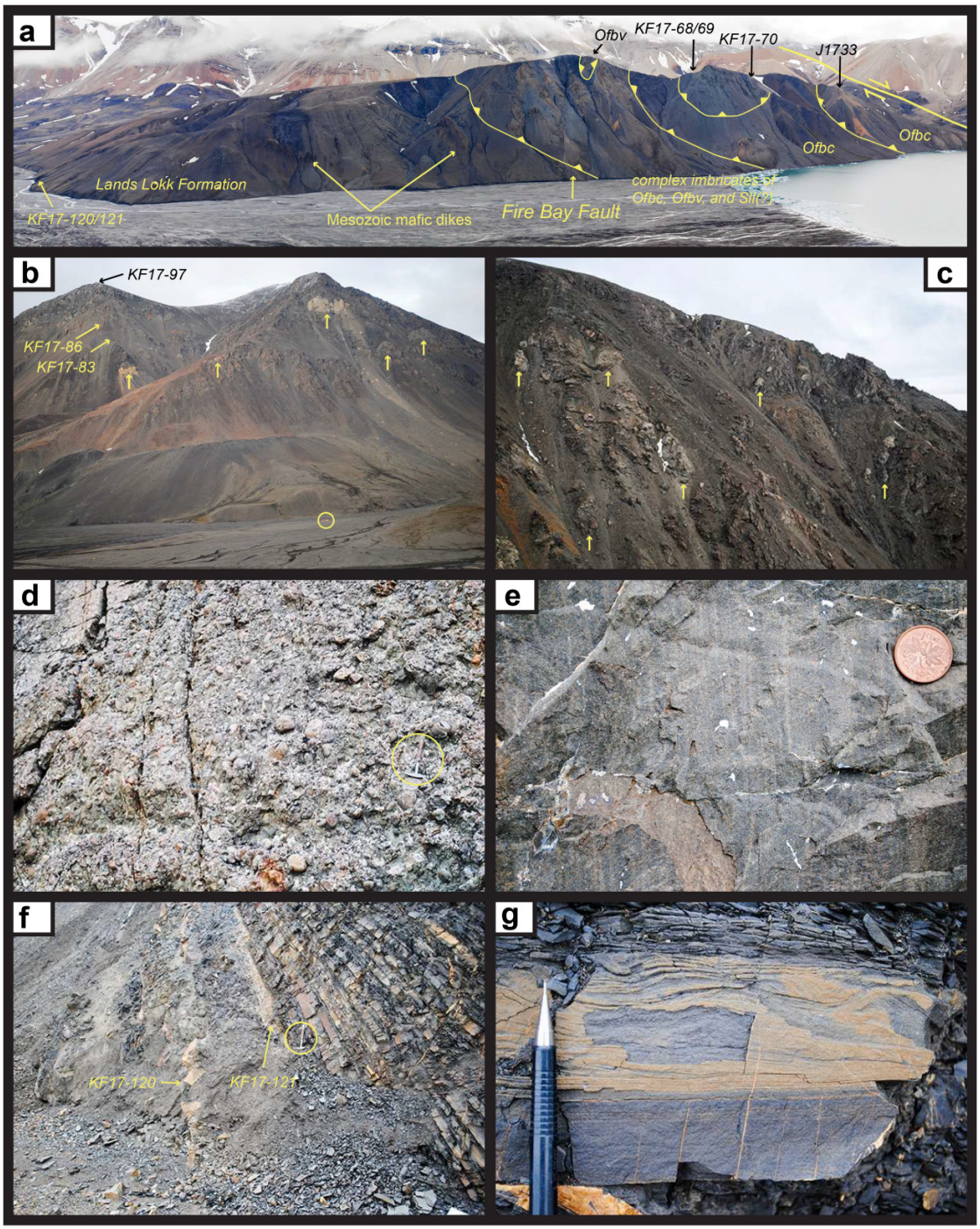

and are locally cut by younger Mesozoic dikes (Fig. 2). As highlighted above, the Fire Bay fault was originally recognized by Trettin (1969) as a major lithological boundary separating different members of the Lands Lokk Formation, and later as a transition between facies belts of the Fire Bay Formation (Trettin 1998). In contrast, Trettin and Nowlan (1990) proposed this as a structural boundary between the Ordovician Fire Bay assemblage and the Silurian Lands Lokk Formation; our observations support the latter definition.

Deformation within the northern imbricate fault panels is variable and complex, consisting of chaotic zones of broken formation and more coherent intervals with shallowly plunging, open to tight, asymmetric, rounded to chevron folds with vertical to steeply dipping, NE-striking hinge planes. Most volcanic and coarse-grained clastic rocks in these fault panels record multiple cleavages, whereas finer grained units either contain a prominent slaty cleavage or more complex cleavage refraction patterns. On the west side of Fire Bay (Fig. 2), most of Trettin's (1998) Member B volcanic- and volcaniclastic-dominated packages form discontinuous lens-shaped fault slivers or tectonic mélange hosted within finer grained packages of siliciclastic strata (Fig. 6*a*), while on the eastern side of the bay there are thick exposures of fault-bounded volcanic and volcaniclastic rocks (Figs. 6*b* and 6*c*). In addition to Trettin's (1998) detailed descriptions of these units (his Hazen Formation and northwestern facies of Members A and B of the Fire Bay Formation), we also observed (1) multiple intervals of massive to crudely stratified clast-supported volcaniclastic conglomerate with volcanic, plutonic, and sedimentary lithic clasts (Fig. 6*d*); (2) >50 m thick packages of pillow basalt and intermediate to mafic flows and breccia (Fig. 6*e*); and (3) massive units of olistostromal matrix-supported conglomerate and sedimentary mélange with up to 100 m long rafts of carbonate, volcanic, and plutonic lithologies (Figs. 6*b* and 6*c*). The latter two of these facies are only exposed in significant peaks on the eastern side of Fire Bay (Figs. 2 and 6*b*).

All of the available fossil age controls from the northern imbricate belt (Fig. 2, sites F1–3 and 6) are from carbonate olistoliths and graptolitic shale units that indicate an Early–Late Ordovician (Floian–Sandbian) depositional age (Trettin and Nowlan 1990; Trettin 1998). We collected an additional conodont sample from a >5 m wide recrystallized limestone olistolith (sample J1732, Fig. 2) and graptolites from dark grey cherty slate in an adjacent fault panel (sample J1733, Figs. 2 and 6*a*). Both of these collections yielded similar age faunas to previous reports summarized in Trettin (1998): (1) Darriwilian conodonts, including specimens of *Cordylodus horridus*, *Histiodella* sp., *Juanognathus* sp., *Microzarkodina* sp., *Periodon* sp., and *Protopanderodus* sp. (Nowlan 2019) and (2) Sandbian graptolites of the *Climacograptus bicornis* zone (Fig. 5, see Supplementary Data S9). In addition to these fossil constraints, a detrital zircon U/Pb sample harvested from the GSC archives (C-242744 of the Fire Bay Formation; Fig. 3; Beranek et al. 2015) has an Ordovician youngest single grain age of 474 ± 10 Ma (2σ).

South of the Fire Bay fault, Trettin (1998) identified a large swath of his southeastern facies of Member A of the Fire Bay Formation, along with limited exposures of the Hazen Formation (Trettin 1996). Three dispersed graptolite collections define the age relationships in this region, including two Middle to Late Ordovician localities (F4 and F5, Fig. 2; Hazen Formation of Trettin 1998) and one Silurian (early late Llandovery) site (F12, Fig. 2; Fire Bay Formation of Trettin 1998). We revisited these localities and found the Silurian graptolite locality to be hosted in a well-exposed succession of overturned thin- to medium-bedded lithic arenite interbedded with fossiliferous calcareous siltstone and shale. In contrast, site F4 is located in a large block of loose talus at the base of a hillside with no clear relationship to surrounding in situ outcrops and site F5 is located in a fault-bounded panel with exposures limited to chert and shale screen at the base of a till-covered drainage. Given the complexity of the regional structural relationships and the presence of widespread sedimentary glacial erratics in the Fire Bay area, we considered these Ordovician fossil localities to be much too ambiguous to precisely define age relationships in the southern clastic-dominated succession.

As described in Trettin (1998), the clastic strata south of the Fire Bay fault are dominated by interbedded lithic arenite, calcareous siltstone, and slaty mudstone with locally abundant tuffaceous mudstone (Fig. 6*f*) and spectacularly preserved turbiditic facies (Fig. 6*g*). Similar to the northern imbricate belt, the coarser grained strata record multiple complex brittle fracture cleavages and the finer grained lithologies contain a prominent slaty cleavage or multiple cleavages. However, the overall structural style differs in this region based on preservation of more coherent packages of broadly folded clastic strata and limited evidence for broken formation or pervasive fault imbrication (Fig. 6*a*). Given the similarity of these strata to widespread exposures of the Lands Lokk Formation directly along strike to the east (Trettin 1996; Trettin and Mayr 1996) and the presence of unambiguous Llandovery graptolites in well-preserved outcrops, we suggest all of the rocks south of the Fire Bay fault should be considered the Lands Lokk Formation (Fig. 2) as originally envisioned by Trettin (1969) and Trettin and Nowlan (1990).

U/Pb geochronology

To understand the age relationships and provenance of early Paleozoic rocks in the Fire Bay area, we collected: (1) three igneous clasts from volcaniclastic clast- and matrix-supported conglomerate/olistostrome that were analyzed by SIMS, (2) a volcanic tuff horizon which was analyzed by LA–ICP–MS, (3) a lithic tuff sample analyzed by LA–ICP–MS and CA–TIMS, and (4) multiple lithic arenite and volcaniclastic sandstone samples that were analyzed by LA–ICP–MS for detrital zircon U/Pb geochronology. These samples were selected from outcrops along stratigraphic sections originally mapped by Trettin (1996, 1998) as the Fire Bay Formation, except for one sample that was collected from his Danish River Formation (Fig. 3); below, we use our updated map unit designations cross-referenced with the qualitative sections of Trettin (1998) to describe what units the samples were collected from (Fig. 2).

Fire Bay assemblage volcanic unit

The three intermediate to felsic igneous clast samples in the Fire Bay assemblage yielded elongate euhedral zircon

Fig. 7. Concordia and chondrite-normalized REE plots of zircon analyses from (*a*, *b*) clasts (KF17-86 and KF17-68) in matrix-supported conglomerate of the Fire Bay assemblage, (*c*) an igneous clast (KF17-70) in clast-supported conglomerate of the Fire Bay assemblage, and (*d*) a tuffaceous mudstone layer (KF17-121) in the Lands Lokk Formation. (*e*) Concordia and weighted mean plot of CA–TIMS data from a lithic tuff (KF17-83) in the Fire Bay assemblage. U/Pb data in (*a*–*c*) were acquired at the Stanford-USGS SHRIMP-RG facility and ^{204}Pb-corrected data are plotted at 1σ. Data in (*d*, *e*) were collected at Boise State University and plotted at 2σ. [Colour online.]

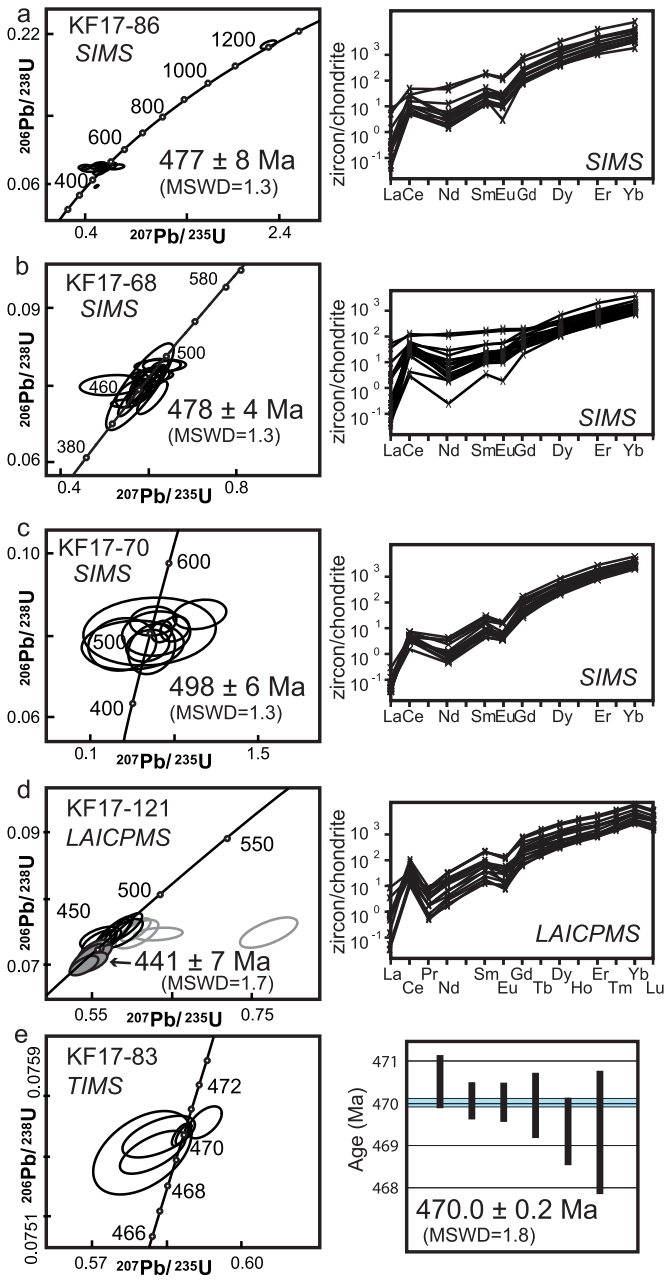

with well-developed oscillatory zoning. First, a rhyolite clast (KF17-86) collected from olistostromal matrix-supported conglomerate in Trettin's (1998) section 2 (Figs. 2–3 and 6*c*; Member B2) yielded ^{206}U/^{238}Pb dates ranging from 1227 to 351 Ma (Fig. 7*a*). The three older grains (502–505 and 1127 Ma) are interpreted as inherited components and the youngest result is inferred to reflect Pb loss. The remaining analyses define a Concordia age of 477 ± 8 Ma with a mean square of weighted deviates (MSWD) of 1.3 (n = 9/13; Fig. 7*a*). Second, an andesitic clast collected from a clast-supported conglomerate in Trettin's section 1 (KF17-68; Figs. 2–3 and 6*a*; Member A3) defined a similar Concordia age of 478 ± 4 Ma (MSWD = 1.3; n = 16/20), assuming three older analyses (490–568 Ma) record inheritance and a single younger analysis (445 Ma) reflects Pb loss (Fig. 7*b*). Finally, a diorite clast (KF17-70; Figs. 2–3 and 6*d*) was collected from an ~5 m thick clast-supported conglomerate in the uppermost part of Trettin's (1998) section 1 (Member A4). This clast yielded a slightly older Cambrian age with a ^{206}Pb/^{238}U weighted mean age of 498 ± 6 Ma (MSWD = 1.3; n = 15/15; Fig. 7*c*). Zircon trace element results from these samples show typical igneous patterns (Hoskin and Schaltegger 2003), while zircon from the andesite clast sample (KF17-68) has elevated light rare earth elements suggestive of alteration. Ages from these samples are consistent with an Early Ordovician MDA for the Fire Bay assemblage.

Sample KF17-83 of the Fire Bay assemblage was collected from a lithic tuff horizon with prominent flow banding (Fig. 6*e*) in an ~100 m thick volcanic package dominated by mafic to felsic flows and fragmental units in the uppermost part of Trettin's (1998) section 2 of the Fire Bay Formation (Figs. 2–3 and 6*b*; Member B1). Although most of the volcanic rocks we encountered in the Fire Bay assemblage were volcaniclastic, this coherent package demonstrably comprised primary volcanic horizons, including crystal and lithic tuffs, breccias, agglomerates, and flows. Sample KF17-83 yielded euhedral oscillatory zoned zircon that define a unimodal ca. 500–450 Ma age population and define a ^{206}Pb/^{238}U weighted mean age of 474 ± 1 Ma (n = 202; MSWD = 2.0) and MLA of 472 ± 1 Ma (Fig. 8*a*). The TuffZirc algorithm (Ludwig 2008) rejected the three youngest grains and generated an age of 473 ± 1 Ma from 186 analyses. Six grains with dates younger than the LA–ICP–MS weighted mean age were selected on the basis of size and clarity and plucked from the mount for CA–TIMS analysis. The grains gave a weighted mean age of 470.0 ± 0.2 Ma (Fig. 7*e*), which is interpreted as the eruptive depositional age for the lithic tuff. Additional zircon grains with ages ranging from ca. 1794 to 654 Ma reflect recycled input from older sources.

Detrital zircon sample KF17-69 was collected from a volcaniclastic lithic arenite horizon in Fire Bay section 1 of Trettin (1998) (Figs. 2–3 and 6*a*; Member A3). The sample yielded a diverse population of euhedral to well-rounded, elongate to equant zircon grains. Euhedral grains display well developed oscillatory zoning. Rounded subequant grains have variable zoning patterns that are commonly truncated at the grain boundaries (Supplementary Data S6). Approximately 65% (n = 212/311) of the analyses pass the discordance filters and 50% of those range from 497 to 441 Ma, defining consistent MDA estimates based on an MLA of 466 ± 2 Ma (Fig. 8*a*) and TuffZirc age of 466 ± 1 Ma (n = 99; rejecting the two youngest analyses). The Ordovician ages are largely derived from oscillatory zoned euhedral grains. Grains with older ages ranging from ca. 3115 to 497 Ma define broad peaks at ca. 615–500, 1200–1000, 1365, 1950–1625, and 3000–2500 Ma.

Fig. 8. (*a*) Probability density plots showing the distribution of zircon ages for detrital samples KF17-69, KF17-97, KF17-105A, KF17-120, and lithic tuff sample KF17-83. Probability density plots in grey show U/Pb data from Beranek et al. (2015). Maximum likelihood ages (MLAs) calculated with Vermeesch (2018*b*). Unmix ages calculated with Ludwig (2008). (*b*) Hf isotopic data from detrital samples KF17-69, KF17-97, KF17-120, KF17-83, C242744, and C242700 and clast samples KF17-68, KF17-70, and KF17-86 compared with Hf data from Ordovician units in the Pearya terrane and Clements Markham belt reported by Malone et al. (2019). Curves for depleted mantle (DM) array and chondritic uniform reservoir (CHUR) are adapted from Vervoort and Blichert-Toft (1999) and Bouvier et al. (2008), respectively. [Colour online.]

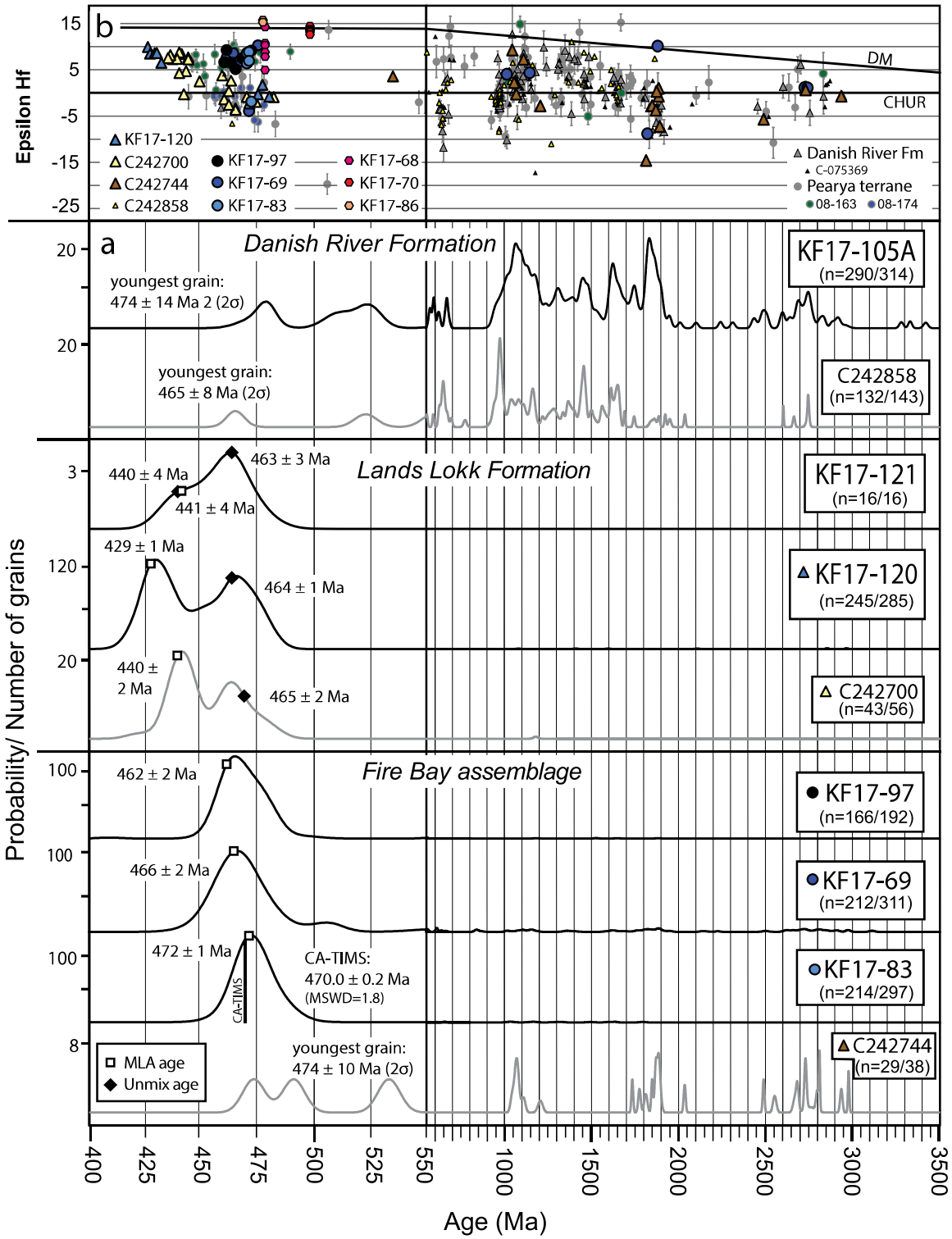

Sample KF17-97 was collected from an ~2 m thick volcaniclastic lithic arenite interbedded with pillow basalts and breccias of the Fire Bay assemblage at the top of section 2 of Trettin (1998) (Figs. 2–3 and 6*b*; Member B2). The sample contained a small population of elongate, euhedral to subhedral grains with well-developed oscillatory zoning. Detrital zircon ages define a dominant peak with ages ranging from ca. 498 to 449 Ma with another five analyses ranging from 1882 to 554 Ma (Fig. 8*a*). The ca. 498–449 Ma population ($n = 146$) gives a $^{206}Pb/^{238}U$ weighted mean age of 468 ± 1 Ma (MSWD = 3), MLA of 462 ± 2 Ma and TuffZirc age of 466 ± 2 Ma ($n = 115$; rejecting 10 youngest grains). The MLA is interpreted as the best estimate for the MDA of the unit sampled.

Lands Lokk Formation

Sample KF17-120 was collected from an ~30 cm thick lithic arenite bed in turbiditic and tuffaceous strata from the Lands Lokk Formation in Trettin's (1998) section 5 (Figs. 2–3 and 6*f*; originally considered the southeastern facies of Member A4 of the Fire Bay Formation). The sample contained a population of euhedral oscillatory zoned grains that yielded ages ranging from 480 to 418 Ma with 6 of 194 grains providing detrital ages >1000 Ma. The population defines peaks at 430 ± 1 Ma and 464 ± 1 Ma determined by the Unmix algorithm (Fig. 8*a*). The younger peak provides a TuffZirc age of 431 ± 2 Ma ($n = 97$; rejecting seven youngest grains) and an MLA of 424 ± 3 Ma, which suggests a Ludlow (Silurian) MDA for this unit. The U/Pb age distribution from the sample is similar to that observed for a sample of volcanic lithic conglomerate (C-242700) reported in Beranek et al. (2015) from the Fire Bay Formation (Fig. 2). Sample C-242700 yielded Unmix ages of 440 ± 2 and 465 ± 2 Ma with an MLA of 438 ± 2 Ma (Fig. 8*a*).

Sample KF17-121 was collected from tuffaceous mudstone ~70 cm above sample KF17-120 within the Lands Lokk Formation (originally mapped in Trettin's (1998) southeastern facies of Member A of the Fire Bay Formation; Figs. 2–3 and 6*f*). This sample yielded U/Pb dates ranging from 471 to 435 Ma with a subtle younger peak defined by the four youngest grains that give a weighted mean $^{206}Pb/^{238}U$ age of 441 ± 7 Ma (MSWD = 1.7; $n = 4/16$; Fig. 7*d*) and MLA of 441 ± 4 Ma (Fig. 8*a*). The Unmix function of Isoplot (Ludwig 2008) provides peak ages of 440 ± 4 and 463 ± 3 Ma. The older peak is interpreted to represent detrital components incorporated into the tuffaceous mudstone whereas the younger peak age is consistent with the MLA, which is interpreted as the best estimate of the MDA for the unit.

Danish River Formation

Sample KF17-105A is a micaceous lithic arenite collected from well exposed turbiditic strata of the Danish River Formation (Figs. 2–3, 4*b*, and 4*c*). The zircon grains are rounded to euhedral and show variable CL zoning patterns, including well-developed oscillatory zoning, coarse patchy zoning, and clear cores overgrown by zoned to unzoned rims. The detrital U/Pb signature is dominated by Precambrian ages between ca. 2000 and 1000 Ma as well as a broad distribution of ages from approximately 700 to 500 Ma. The Precambrian ages are similar to the minor Precambrian signature observed in sample KF17-69 of the Fire Bay assemblage; however, this sample lacks the dominant ~480–465 Ma Ordovician signature documented in the other Fire Bay and Lands Lokk detrital and igneous zircon samples (Fig. 8*a*). The youngest zircon ages are ca. 474 ± 7 and 480 ± 4 Ma, and the broader detrital signature is consistent with results from the Danish River Formation reported by Beranek et al. (2015) from sample C-242858 in the Emma Fiord Fault Zone (Figs. 2 and 8*a*).

Zircon Hf isotope geochemistry

Zircon Hf isotope results from the Fire Bay assemblage and the Lands Lokk and Danish River formations are divided into samples that define Ordovician unimodal peaks and those that define both Ordovician and Silurian peaks (Fig. 8*b*). Zircon from samples with unimodal peaks at ~470–465 Ma define a cluster of positive εHf values ranging from +5.2 to +10.3 with only 2 of 17 analyses as outliers at −1.9 and −3.9. Similarly, Cambrian and Ordovician grains from clasts within Fire Bay assemblage units are consistently juvenile with εHf of +5.0 to +15.8 (Fig. 8*b*). Ordovician grains in samples with two Paleozoic peaks (e.g., KF17-120 of the Lands Lokk Formation) record εHf values of −2.3 to +1.6 that is distinct from the juvenile signature of Ordovician grains in the Fire Bay assemblage, whereas Silurian grains record juvenile εHf values from +6.4 to +10.0. Hafnium isotopic results from sample C-242700 of Beranek et al. (2015) connect the more evolved cluster at ca. 479 Ma and the juvenile cluster at ca. 430 Ma. Precambrian grains analyzed from samples KF17-69 and C-242744 (Beranek et al. 2015) overlap with εHf values observed for age equivalent grains in the Silurian Danish River Formation elsewhere in the Clements Markham belt (Fig. 8*b*; sample C-075369, Malone et al. 2019).

Igneous geochemistry

Fire Bay assemblage volcanic unit

Six samples of mafic to felsic volcanic flows and tuffs and four samples of pillow basalt were collected from volcanic units within the Fire Bay assemblage (Members B1 and B2 of the Fire Bay Formation of Trettin 1998) along a traverse up a prominent peak on the eastern side of Fire Bay (Figs. 2 and 6*b*). Five additional intermediate to felsic plutonic and volcanic clasts were collected from volcaniclastic conglomerates exposed on both sides of Fire Bay, three of which were dated with U/Pb geochronology (Figs. 2–3, 6*c*, and 6*d*). The flows and tuffs are dominated by a matrix of altered glass that surrounds plagioclase, K-feldspar, and quartz phenocrysts with many primary silicate minerals replaced by chlorite or calcite. The reworked plutonic clasts have interlocking crystals of plagioclase, K-feldspar, and quartz with chlorite replacing biotite. Representative photomicrographs of these volcanic and plutonic samples are included in Supplementary Data S10.

The Fire Bay assemblage flows and tuffs range in composition from basalt to rhyolite (Zr/Ti = 0.01–0.07; Fig. 9*a*) on the Pearce (1996) classification diagram. The igneous clasts generally have elevated Zr/Ti ratios, indicating an evolved composition (Fig. 9*a*). In contrast, pillow basalts in the uppermost part of the volcanic unit of the Fire Bay assemblage have a similar Zr/Ti ratio (ranging from 0.01 to 0.02) but record elevated Nb/Y values, suggesting higher alkalinity melts (Fig. 9*a*). The samples show a wide range of Sc values (Sc = 5–30 ppm) that decrease with increasing Zr content (Fig. 9*b*), and a similar trend can be observed for Ti with the evolved igneous clasts plotting towards the end of fractionation trend (Fig. 9*c*). Combined, these trends are indicative of fractionation of plagioclase, pyroxene, and amphibole with some likely role of assimilation (e.g., Pearce and Norry 1979).

All of the volcanic and plutonic samples are enriched in light rare earth elements (LREE) with respect to heavy rare earth elements (HREE) (Fig. 9*d*). $La_{[PM]}/Yb_{[PM]}$ ratios vary from 1 to 4 in the mafic to felsic Fire Bay assemblage flows and tuffs, and increase within the pillow basalts to 6–8. The flows, tuffs, and volcanic and plutonic clasts also show elevated Th contents with respect to Nb and Ta (Fig. 9*d*, $Nb^* = 0.1–0.7$; calculated as $Nb_{[PM]}/(Th_{[PM]} \cdot La_{[PM]})^{0.5}$), and a similar negative Nb anomaly is recorded in the overlying pillow basalts ($Nb^* = 0.4–0.5$). Igneous εNd values are consistently positive (+1.4 to +2.8) among all of the Fire Bay samples, while the $^{87}Sr/^{86}Sr$ ratios are lowest in the Fire Bay pillow basalts (~0.7048) and increase to 0.7063–0.7078 in the flows and plutonic clasts (Fig. 9*e*).

Based on normalization to primitive mantle compositions, igneous flows and tuffs record a pattern characteristic of arc-related rocks (Fig. 10*a*), such as in the Marianas arc (Pearce et al. 2005). On the Th/Yb–Nb/Yb diagram of Pearce (2008), the samples show elevated Th/Yb ratios (0.1–6.3) with respect to the mantle array, indicating influence from a subduction component or interactions with the subcontinental lithosphere (Fig. 10*b*). The Fire Bay pillow basalts have elevated Nb/Yb, indicating an enriched mantle source, but also higher Th/Yb (Fig. 10*b*). The Ti/V ratios from mafic to felsic flows and tuffs range from 13 to 29 with one sample having a Ti/V = 78 (Fig. 9*c*), which are characteristic of an arc setting (Shervais 1982, 2022). In contrast, the Fire Bay pillow basalts have high Ti/V between 94 and 119, with one sample having a Ti/V = 56.

Danish River(?) volcanic rocks

Seven samples were collected from pillow basalts and dikes within the Danish River(?) volcanic rocks unit in the northern Fire Bay area (Figs. 2 and 4*d*). The samples are highly altered, and pseudomorphs after olivine and pyroxene are entirely replaced by calcite or chlorite. The moderate to significant degree of alteration in these early Paleozoic rocks prohibits reliable use of major elements, so immobile trace elements are used in the geochemical assessment below (e.g., Winchester and Floyd 1977).

Danish River(?) pillow basalts and dikes have higher Nb/Y ratios, ranging between 2.7 and 4.7, and plot within alkali basalt or foidite fields (Fig. 9*a*). Compared to the Fire Bay assemblage, these samples show less variation in trace element concentrations and have elevated Zr and Ti concentrations more characteristic of within plate basalts (Pearce 1982). The samples cluster together around a Ti/V value of 50 (Fig. 10*c*), which is indicative of an alkaline composition in either a back-arc or oceanic island basalt (OIB) setting (Shervais 1982, 2022).

The Danish River(?) samples are enriched in LREE with respect to HREE (Fig. 9*d*) and have elevated $La_{[PM]}/Yb_{[PM]}$ of 15–25. Nb and Ta are both elevated compared to Th and La (Fig. 9*d*, $Nb^* = 1.3–1.6$). Mafic rocks preserve characteristics of OIBs when normalized to primitive mantle compositions (Fig. 10*a*). The Danish River(?) volcanic rocks plot along the mantle array in a field of alkali basalts and OIB on a Th/Yb–Nb/Yb diagram (Fig. 10*b*).

Discussion

The combined geochronologic results reflect a prolonged magmatic history recorded by early Paleozoic clastic and volcanic units in the Emma Fiord region of the Clements Markham belt in northern Ellesmere Island. These new data divide the units into three age categories: (1) clasts derived from pre-Ordovician sources, (2) Ordovician volcanic, volcaniclastic, and clastic units, and (3) Silurian clastic and volcaniclastic units with lesser mafic volcanic layers. The data combined with the field relationships and biostratigraphic results described above require revisions to the stratigraphic architecture of the field area. Specifically, we propose abandoning the local use of "Hazen Formation" and "Fire Bay Formation" in exchange for the previously defined Fire Bay assemblage of Trettin and Nowlan (1990). The complexly deformed Lower–Upper Ordovician Fire Bay assemblage is separated from lower Silurian clastic rocks of the Lands Lokk Formation to the south along the newly defined Fire Bay fault (Figs. 2 and 3), although there may be imbricated slivers of the two units within the fault zone. To the north, we propose that Trettin's (1998) Member C of the Fire Bay Formation is instead part of the Lands Lokk and/or Danish River formations (Figs. 2 and 3). Critically, these suggestions posit that the Fire Bay assemblage is a structurally modified Ordovician unit with distinct volcanic- and sedimentary-dominated successions but no clear facies belts (sensu Trettin 1998) and no unambiguous evidence for Silurian magmatism and/or sedimentation.

The best age estimates for the volcanic and clastic units of the Fire Bay assemblage (Fig. 3) are provided by the newly dated lithic tuff (KF17-83), which gave an age of 470.0 ± 0.2 Ma, and new and previous collections of Floian–Sandbian conodonts and graptolites (Trettin 1998; Nowlan 2019). The new U/Pb data collectively define a robust record of ca. 480–450 Ma magmatism in volcanic and clastic units of the Fire Bay assemblage and suggest an Early to early Late Ordovician depositional age for the unit as a whole. Zircon and whole-rock isotope and trace element geochemical results indicate that the Fire Bay assemblage volcanic rocks formed in a relatively juvenile oceanic arc setting. The pillow basalts in the Fire Bay volcanic unit record enrichment in LREE along with positive εNd values and high Nb/Yb and Ti/V ratios that

Fig. 9. Whole-rock major and trace element geochemistry of igneous samples collected in the Fire Bay area. (*a*) Classification diagram based on the Zr/Ti versus Nb/Y ratios after Pearce (1996); symbols in legend used in all plots. (*b*) Log–log plot of Sc and Zr concentration, solid lines indicate fractionation vectors, dashed lines indicate fractionation of plagioclase, amphibole, and clinopyroxene. The fractionation trajectories and vectors were calculated using the coefficients from Rollinson (1993) for andesitic magmas and a starting composition of the sample with the lowest Zr concentration (sample KF17-76B). Note that fractionation trajectories do not take into account assimilation. (*c*) Log–log plot of Ti versus Zr concentration, fractionation trends calculated the same way as for B). (*d*) Trace element data normalized to Primitive Mantle composition (Sun and Mcdonough 1989); inset shows the ratio of normalized Yb plotted against Nb* anomaly calculated as $Nb_{[PM]}/(Th_{[PM]} \cdot La_{[PM]})^{0.5}$. (*e*) Plot of whole-rock $\varepsilon Nd_{(t)}$ versus $^{87}Sr/^{86}Sr_{(i)}$ for igneous clasts of the Fire Bay assemblage. Abbreviations: Am, amphibole; Cpx, clinopyroxene; Ol, olivine; Opx, Orthopyroxene; Pl, plagioclase. [Colour online.]

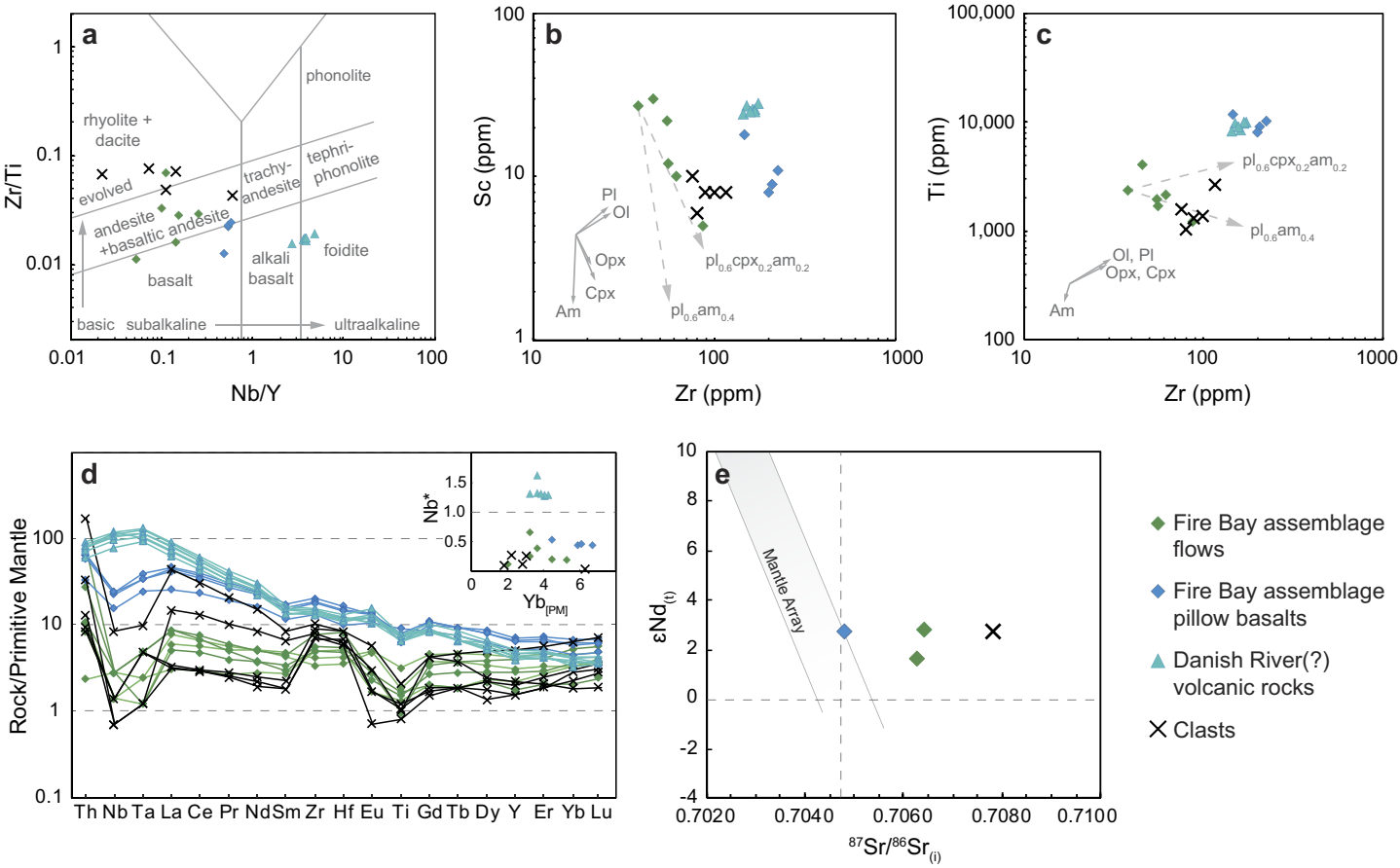

are more consistent with being sourced from an enriched mantle wedge above a subduction zone or back-arc basin setting (Shervais 1982; Saunders and Tarney 1984; Piercey et al. 2002; Pearce et al. 2005). Since back-arc basin basalts display a wide range of compositions, from LREE-enriched to -depleted with various crustal or subduction related components (e.g., Taylor and Martinez 2003), the setting remains ambiguous based on trace element data alone (e.g., Li et al. 2015; Saccani 2015; Gill et al. 2021). The volcanic, sedimentological, and structural characteristics of the Fire Bay assemblage are compatible with a juvenile forearc basin and accretionary prism setting as well.

The ~480–450 Ma range of Fire Bay assemblage volcanism overlaps with the age of arc-related plutonic rocks in the Pearya terrane and volcanic rocks in the eastern Clements Markham belt (Trettin et al. 1998; Malone et al. 2019). MDAs from the two volcaniclastic samples are consistent with a Darriwilian age for the volcanic member of the Fire Bay assemblage (Fig. 11). In addition, ages from igneous clasts in volcaniclastic conglomerate provide additional support for nearby Early Ordovician magmatism, and the older clast age of 498 ± 6 Ma may indicate input from older juvenile magmatic sources such as volcanic rocks of the Yelverton or Jaeger Lake formations in the Clements Markham and Northern Heiberg belts, respectively, or the Pearya terrane (Fig. 1; Trettin 1998). Detrital zircon data compiled from Ordovician and Silurian units in the Pearya terrane, Fire Bay area and the remaining Clements Markham and Northern Heiberg belts define four signatures characterized by: (A) a Paleozoic peak representative of Ordovician and/or Silurian magmatism; (B) prominent Ordovician–Silurian peaks with lesser Paleoproterozoic peaks; (C) a dominant Tonian peak with minor Ordovician–Silurian and older Precambrian peaks; and (D) broad Mesoproterozoic spectra with variable Silurian–Ordovician peaks (Fig. 12*a*).

Fig. 10. Comparison of whole-rock geochemical signatures of samples collected in the Fire Bay area to those from specific tectonic settings. Symbols are the same as in Fig. 9. (*a*) Trace element data normalized to primitive mantle composition (Sun and Mcdonough 1989). The range of values from analyzed samples is compared to the composition of oceanic island basalt (OIB), upper continental crust (UCC), enriched mid-oceanic basalt (EMORB), normal mid-oceanic basalt (NMORB), and the Mariana Arc. Data for OIB, EMORB, and NMORB are from Sun and Mcdonough (1989), UCC from Taylor and McLennan (1995), and the Mariana Arc (average of the southern Seamount Province) from Pearce et al. (2005). (*b*) Nb/Yb versus Th/Yb plot after Pearce (2008). Abbreviations: AFC, assimilation–fractional crystallization; SZ, subduction input. (*c*) Ti/V tectonic discrimination plot after Shervais (1982). (*d*) Ta/Yb discrimination plot for plutonic rocks after Pearce et al. (1984). [Colour online.]

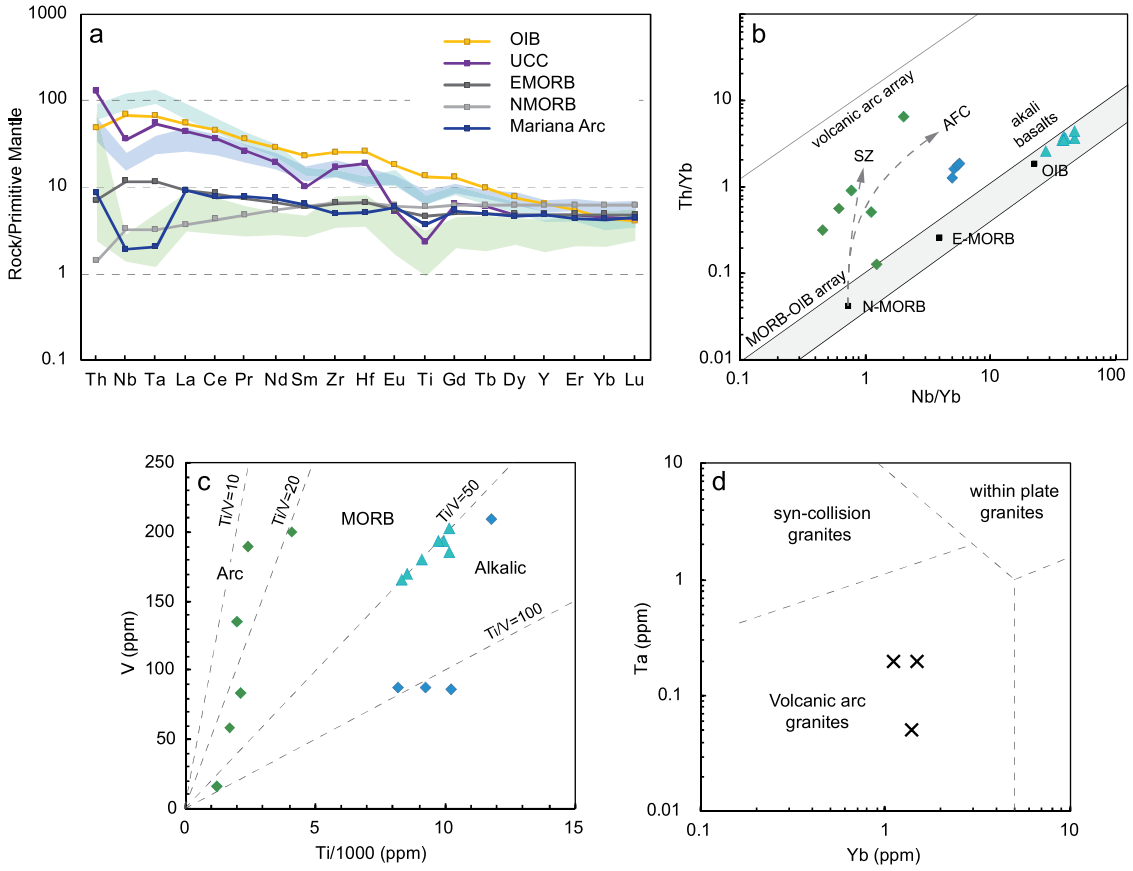

Fig. 11. Summary of new age control on the depositional ages of the Fire Bay assemblage and the Lands Lokk and Danish River formations in the Fire Bay area of Emma Fiord using the timescale of Walker et al. (2018). MDA, Maximum depositional age (MDA) and maximum likelihood age (MLA) calculated with Vermeesch (2018*b*). TuffZirc and Unmix ages calculated with Ludwig (2008).

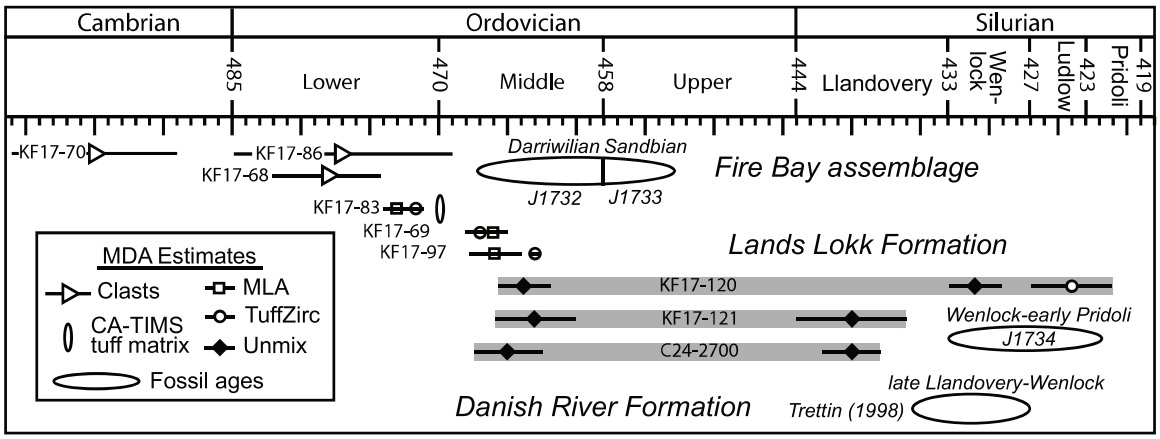

Fig. 12. Three-dimensional multidimensional scaling (MDS) plots of U/Pb detrital zircon data. (*a*) Comparison of Ordovician and Silurian samples from Fire Bay, Pearya terrane, and Clements Markham and Northern Heiberg belts defining distinct age groups, A–D. Data from (*a*) are combined by location and age group (A–D) and compared with (*b*) Ordovician and (*c*) Silurian units in arc terranes of the circum-Arctic and Cordilleran regions. The MDS plots use a Kolmogorov–Smirnov comparison generated with the DZmds routine of Saylor et al. (2017). Shepard plots, probability density plots of samples used to define groups A–D, and data references are provided in Supplementary Data S11. [Colour online.]

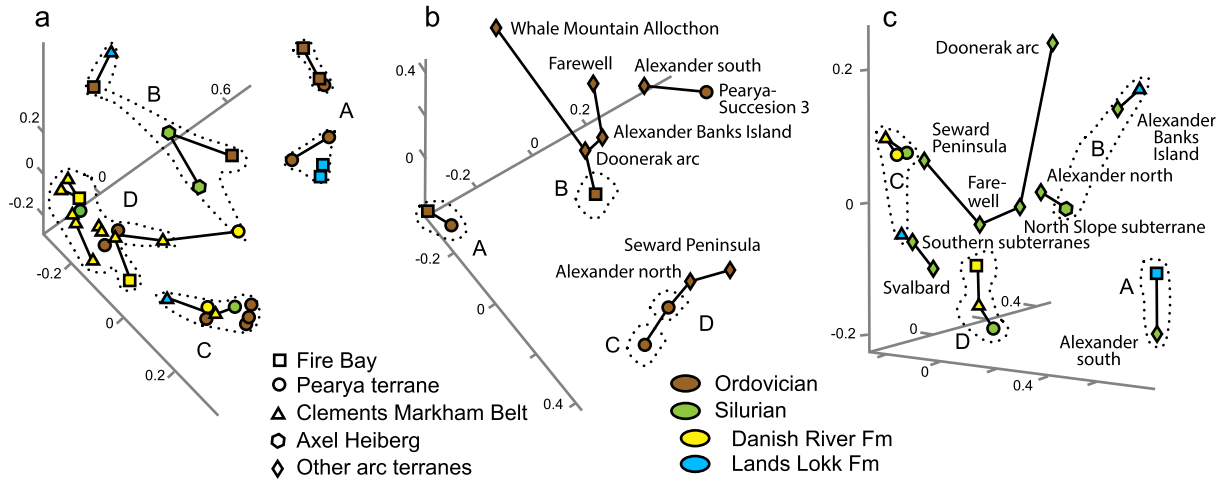

Samples assigned to the Fire Bay assemblage have dominant Ordovician peaks (group A) and in some cases, input from older sources (group B). Pearya terrane samples from the Cape Discovery Formation and lower Taconite River Formation have a similar detrital zircon signature, but samples from the upper Taconite River, Cranstone and Lorimer Ridge formations show an increase in Tonian grains (group C) and an influx of Mesoproterozoic grains (group D). The Maskill complex of Pearya's Succession 3 is dominated by a ca. 575 Ma detrital zircon signature (Estrada et al. 2018) that is lacking in the Fire Bay assemblage. Expression of the Tonian signature that dominates much of the Pearya terrane record (e.g., Malone et al. 2019) is also minimal in the Fire Bay assemblage. The juvenile zircon Hf isotope signature of the Fire Bay volcaniclastic units is compatible with a sample of the Taconite River Formation in the Pearya terrane (08-163, Malone et al. 2019), but Ordovician units of the Pearya terrane have a higher abundance of zircon grains with more evolved Hf values (Fig. 7).

The apparent differences in detrital zircon age and Hf signature indicate that the Fire Bay assemblage most likely does not share the same arc basement with the Pearya terrane; however, primary ties cannot be ruled out due to the similarity with units of the Pearya terrane that lack Precambrian components (group A). Proximity to the Pearya terrane is consistent with the age of older volcanic components—a felsic unit within Succession 2 of the Pearya terrane (unit M4 of Trettin 1998) yielded a U/Pb zircon age of 503 +8/−2 Ma (Trettin et al. 1987) that is consistent with the age of older volcanic clasts in the Fire Bay assemblage conglomerate horizons. Thus correlation of the Fire Bay assemblage with portions of the Pearya terrane is permissible.

Looking at the broader array of circum-Arctic Ordovician arc signatures, it appears that Fire Bay assemblage units are compatible with the Doonerak arc complex of the Arctic Alaska terrane in the central Brooks Range of Alaska (Fig. 12*c*). The juvenile zircon Hf signatures of both the Fire Bay assemblage and the Apoon assemblage (Strauss et al. 2017) supports evolution in a comparable setting and possible along-strike correlation on a common subduction boundary. The close similarity of some units of the Pearya terrane with the Fire Bay assemblage and Doonerak arc suggests that the Fire Bay assemblage may have evolved in an intraoceanic arc setting between the Pearya terrane and Doonerak arc (Fig. 13). This Ordovician arc complex may record the northern continuation of the convergent boundary responsible for closure of the Iapetus Ocean and Laurentia–Baltica collision (Strauss et al. 2017; McClelland et al. 2022).

Units assigned to the Lands Lokk Formation in the Fire Bay region are characterized by dominant Ordovician peaks similar in age to those of the Fire Bay assemblage combined with significant input of Silurian zircon. The best estimates of the depositional age of the Lands Lokk Formation in the study area are the Ludlow MDA of 438 ± 2 Ma (KF17-120) and Wenlock to lower Pridoli graptolite ages (J1734) from volcaniclastic and clastic rocks within the section, respectively (Fig. 11). Ordovician zircon from the Lands Lokk samples have εHf values that are more evolved than similar age grains in the Fire Bay assemblage and more compatible with the signature of Ordovician units in the Pearya terrane (Fig. 7). This relationship suggests that there are either more evolved sources in the Fire Bay assemblage than are currently recognized, or the Lands Lokk Formation received input from the Pearya terrane or other more distal terranes. The Lands Lokk Formation regionally has a diverse detrital zircon signature that likely reflects variation in local sources that are most similar to other circum-Arctic terranes (Fig. 12), suggesting that the latter may be the case.

Fig. 13. Schematic paleogeographic reconstruction showing the inferred location of the Fire Bay assemblage (FB) relative to other Ordovician arc fragments in the circum-Arctic region. Modified after McClelland et al. (2022). Arctic Alaska: N, North Slope subterrane; SS-SP, southern Brooks Range and Seward Peninsula; Ch, Chukotka of the southwestern subterranes; D, Doonerak; WMA, Whale Mountain Allochthon. AT, Alexander terrane (ATn—northern, St. Elias; ATs, southern, Prince of Wales Island; ATb, Banks Island assemblage); F, Farewell terrane; P, Pearya terrane; S–K, Sierra–Klamath terranes; Sv, Svalbard. [Colour online.]

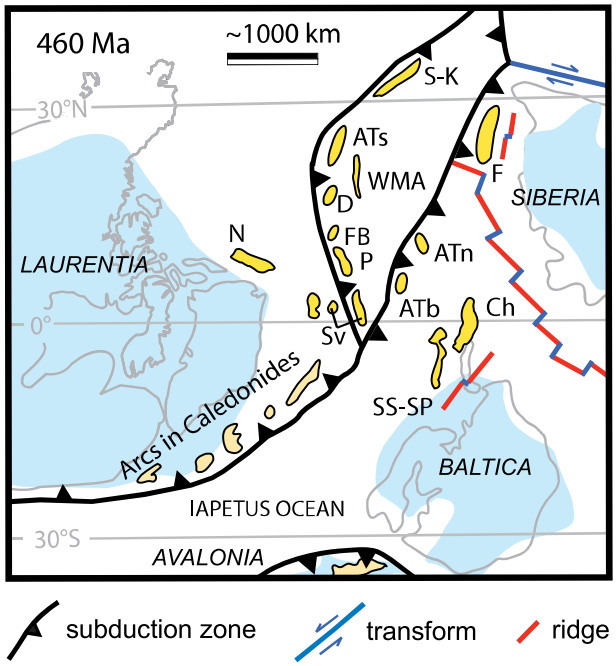

The Danish River Formation in the Emma Fiord region shows an influx of Neoproterozoic and Mesoproterozoic detritus (group D) that is similar to some portions of the Danish River Formation in the Clements Markham belt and the Pearya terrane (Fig. 12; Hadlari et al. 2014; Beranek et al. 2015; Malone et al. 2019). The regional variation in the Danish River Formation signature results from variable input of Tonian zircon (group C) likely derived from the Pearya terrane. The MDA estimates for the Danish River Formation can only be derived from youngest single grain ages of 474 ± 14 (2σ) for this study (Fig. 7) and 465 ± 8 (2σ) from Beranek et al. (2015). These Ordovician estimates are significantly older than the late Llandovery to Wenlock fossil ages reported regionally from the Danish River Formation (Fig. 11), suggesting that Silurian clastic rocks are largely derived from recycling local sources rather than the abundant Silurian arc sources in the circum-Arctic region (Fig. 12).

Mafic magmatism recorded by the Danish River(?) volcanic rocks is assumed to be synchronous with the deposition of Danish River Formation clastic strata. The trace element composition of these mafic rocks indicate an alkalic character that is consistent with enriched lithospheric or asthenospheric sources (Fig. 10). Alkalic magmatism with OIB characteristics can be indicative of an ensialic back-arc rift or back-arc basin setting (e.g. Piercey et al. 2002). Alternatively, rare OIB magmas with alkalic characteristics intruding turbiditic clastic deposits have been reported from transtensional strike–slip settings (Mitjavila et al. 1997), where a diverse set of magmas are generated through tectonically driven decompression melting of various intensities (Mitjavila et al. 1997; Vaughan and Scarrow 2003). The latter setting agrees well with regional models for oblique collision between the Pearya terrane and Franklinian margin of northern Laurentia (Trettin 1998; Malone et al. 2017, 2019; McClelland et al. 2022).

Conclusions

The new field, geochronologic, geochemical, and biostratigraphic data presented here from the Emma Fiord region of northern Ellesmere Island permits modification of previous tectonic models for accretion of the Pearya terrane that are based on a Silurian magmatic age for the Fire Bay assemblage (or Fire Bay Formation of Trettin 1998). These data require an Ordovician depositional age for the Fire Bay assemblage and suggest that it may have formed in an intraoceanic arc setting intermediate between the Pearya terrane and the Doonerak arc of the Arctic Alaska terrane. Silurian arc magmatism ceased in the Clements Markham belt, but input from more distal Silurian arcs in the circum-Arctic region is recorded by detrital zircon in volcaniclastic strata of the Lands Lokk Formation. Detrital zircon signatures of the Danish River Formation are dominated by Precambrian ages that are inferred to reflect input from local basement sources. These new observations from the Fire Bay area are consistent with tectonic models that argue for oblique collision of an Ordovician arc system in the Late Ordovician – early Silurian followed by sinistral translation of accreted material along the northern Laurentian margin. The presence of an Ordovician arc-related assemblage between Laurentia and the Pearya terrane argues strongly against minimal displacement models in which the Pearya terrane is a simple continuation of the Laurentian margin.

Results of the regional mapping programs conducted by the GSC are summarized in Trettin (1998) and provide the first order understanding of the regional geology of northern Ellesmere Island. Although the number of field-based geological studies has been limited due to the remoteness of the area, results of subsequent detailed studies provide additional documentation of and/or rationale for modification of interpretations based on regional relationships. The changes to stratigraphic nomenclature proposed herein reflect newly documented uncertainty in the correlations envisioned by Trettin (1998) but are consistent with the original field observations and interpretations of Trettin and Nowlan (1990). Additional work is needed to test our proposed changes and advance understanding of the detailed stratigraphic and structural relationships that form the basis of disparate tectonic models for the evolution of northern Ellesmere Island.

Acknowledgements

Fieldwork on northern Ellesmere Island, Nunavut, Canada, was funded and organized by the Bundesanstalt für Geowis-

senschaften und Rohstoffe (BGR) and the Geological Survey of Canada during CASE 19. We thank Karsten Piepjohn at the BGR for invitations to participate in this expedition. Additional funding was provided by National Science Foundation grants EAR-16550152 awarded to JVS and EAR-1650022 awarded to Jane Gilotti, Universtiy of Iowa, and co-PI WCMC, and a Natural Sciences and Engineering Research Council of Canada Discovery Grant to MJM. MMK received support from the Cook Scholarship fund in the Earth and Environmental Sciences Department at the University of Iowa. We gratefully acknowledge Jisou Jin of Western University for contributing brachiopod identifications for this study. We thank Thi Hao Bui and Galen Halverson of McGill University for their assistance with Nd isotopic work, Jahan Ramezani of Massachusetts Institute of Technology for help with igneous $^{87}Sr/^{86}Sr$ isotopic work, and Christopher Fisher at Washington State University (now at University of Western Australia) for zircon Hf isotope analyses. The Arizona Laserchron Facility is supported by NSF grant EAR-1649254. Reviews by Shunxin Zhang, Thomas Hadlari, and Associate Editor Alana Hinchey improved the manuscript.

Article information

History dates

Received: 23 November 2021
Accepted: 25 May 2022
Accepted manuscript online: 9 June 2022
Version of record online: 13 October 2022

Copyright

Author information

Author ORCIDs

William C. McClelland https://orcid.org/0000-0003-2699-4667
Justin V. Strauss https://orcid.org/0000-0003-3298-3227

Author notes

Luke P. Beranek served as an Associate Editor at the time of manuscript review and acceptance; peer review and editorial decisions regarding this manuscript were handled by Alana Hinchey and J. Brendan Murphy.

Supplementary material

Supplementary data are available with the article at https://doi.org/10.1139/cjes-2021-0129.

References

Beranek, L.P., Pease, V., Hadlari, T., and Dewing, K. 2015. Silurian flysch successions of Ellesmere Island, Arctic Canada, and their significance to northern Caledonian Palaeogeography and tectonics. Journal of the Geological Society, **172**: 201–212. doi:10.1144/jgs2014-027.

Beranek, L.P., van Staal, C.R., McClelland, W.C., Israel, S., and Mihalynuk, M.G. 2013*a*.Baltican crustal provenance for Cambrian-Ordovician sandstones of the Alexander terrane, North American Cordillera: evidence from detrital zircon U-Pb geochronology and Hf isotope geochemistry. Journal of the Geological Society, **170**: 7–18. doi:10.1144/jgs2012-028.

Beranek, L.P., van Staal, C.R., McClelland, W.C., Israel, S., and Mihalynuk, M.G. 2013*b*.Detrital zircon Hf isotopic compositions indicate a northern Caledonian connection for the Alexander terrane. Lithosphere, **5**: 163–168. doi:10.1130/L255.1.

Bjørnerud, M.G., and Bradley, D.C. 1992. Silurian foredeep and accretionary prism in northern Ellesmere Island: implications for the nature of the Ellesmerian Orogeny. *In* Proceedings of the International Conference on Arctic Margins: U.S. Mineral Management Service Outer Continental shelf Study MMS94-0040. Thurston and Fujita Anchorage, Alaska, September 1992, University of California Libraries, Berkley, CA, pp. 129–133.

Bouvier, A., Vervoort, J.D., and Patchett, J.D. 2008. The lu-hf and sm-nd isotopic composition of CHUR: constraints from unequilibrated chondrites and implications for the bulk composition of terrestrial planets. Earth and Planetary Science Letters, **273**: 48–57. doi:10.1016/j.epsl.2008.06.010.

Brandes, C., and Piepjohn, K. 2021. Eurekan faults on northern Ellesmere Island, Arctic Canada: from Cenozoic strike-slip tectonics to recent seismicity. Journal of Geodynamics, **144**: 101816. doi:10.1016/j.jog.2021.101816.

Churkin, M., Jr., and Trexler, J.H., Jr. 1980. Continental plates and accreted oceanic terranes. *In* The ocean basins and margins: the Arctic Ocean. *Edited by* Nairn, Churkin, Jr. and Stehli Plenum Press, New York, N.Y. pp. 1–20.

Colpron, M., and Nelson, J.L. 2009. A palaeozoic northwest passage: incursion of Caledonian, Baltican and Siberian terranes into eastern Panthalassa, and the early evolution of the North American Cordillera. Earth accretionary systems in space and time. Cawood and Krönervol. **318**, Geological Society of London, Special Publications, Bath, UK, pp. 273–307. doi:10.1144/SP318.10.

Dewing, K., Hadlari, T., Pearson, D.G., and Matthews, W. 2019. Early Ordovician to early Devonian tectonic development of the northern margin of Laurentia, Canadian Arctic Islands. Geological Society of America Bulletin, **131**: 1075–1094. doi:10.1130/B35017.1.

Dumoulin, J.A., Harris, A.G., Bradley, D.C., and de Freitas, T.A. 2000. Facies patterns and conodont biogeography in arctic Alaska and the Canadian Arctic Islands: evidence against juxtaposition of these areas during early Paleozoic time. Polarforschung, **68**: 257–266.

Estrada, S., Tessensohn, F., and Sonntag, B.L. 2018. A timanian island-arc fragment in north Greenland: the midtkap igneous suite. Journal of Geodynamics, **118**: 140–153. doi:10.1016/j.jog.2018.01.015.

Gill, J., Hoernle, K., Todd, E., Hauff, F., Werner, R., Timm, C., et al. 2021. Basalt geochemistry and mantle flow during early backarc basin evolution: Havre Trough and Kermadec Arc, Southwest Pacific. Geochemistry, Geophysics, Geosystems, **22**(2): e2020GC009339. doi:10.1029/2020GC009339.

Hadlari, T., Davis, W.J., and Dewing, K. 2014. A pericratonic model for the Pearya terrane as an extension of the Franklinian margin of Laurentia, Canadian Arctic. GSA Bulletin, **12**: 182–200. doi:10.1130/B30843.1.

Hall, J. 1847. Descriptions of the organic remains of the lower division of the New York system. Palaeontology of New York, vol. **1**. D. Appleton & Co. and Wiley & Putnam, Albany N.Y.

Harrison, J.C., Lunds, T., Ford, A., Trettin, H.P., Thorsteinsson, R., and Mayr, U. 2015. Geology, tectonic assemblage map of the Nansen sound area, northern Axel Heiberg and western Ellesmere Islands, Nunavut: Geological Survey of Canada. Canadian Geoscience Map **26**, scale 1:500 000.

Hoskin, P.W.O., and Schaltegger, U. 2003. The composition of zircon and igneous and metamorphic petrogenesis. *In* Zircon. *Edited by* Hanchar and Hoskin Mineralogical Society of America Reviews in Mineralogy and Geochemistry. vol. **53**. Chantilly, VA, pp. 27–62.

Klaper, E.M. 1992. The Paleozoic tectonic evolution of the northern edge of North America: a structural study of northern Ellesmere Island, Canadian Arctic archipelago. Tectonics, **11**: 854–870. doi:10.1029/92TC00277.

Lapworth, C. 1876. The Silurian system in the south of Scotland. *In* Catalogue of Western Scottish Fossils. *Edited by* Armstrong, Young and Robertson Blackie & Son, Glasgow.

Li, C., Arndt, N.T., Tang, Q., and Ripley, E.M., 2015. Trace element indiscrimination diagrams. Lithos, **232**: 76–83. doi:10.1016/j.lithos.2015.06.022.

Ludwig, K.R. 2008. Isoplot 3.6. Berkeley Geochronology Center Special Publication. vol. **4**. Berkeley, CA, p. 77.

Majka, J., Kośmińska, K., Bazarnik, J., and McClelland, W.C. 2021. The Ordovician Thores volcanic island arc of the Pearya terrane from northern Ellesmere Island formed on Precambrian continental crust. Lithos, **386–387**: 105999. doi:10.1016/j.lithos.2021.105999.

Malone, S.J., McClelland, W.C., von Gosen, W., and Piepjohn, K. 2017. The earliest Neoproterozoic magmatic record of the Pearya terrane, Canadian High Arctic: implications for Caledonian terrane reconstructions. Precambrian Research, **292**: 323–349. doi:10.1016/j.precamres.2017.01.006.

Malone, S.J., McClelland, W.C., von Gosen, W., and Piepjohn, K. 2019. Detrital zircon U-Pb and Lu-Hf analysis of Paleozoic sedimentary rocks from the Pearya terrane and Ellesmerian fold belt (northern Ellesmere Island): a comparison with circum-Arctic datasets and their implications on terrane tectonics. *In* Circum-Arctic structural events: tectonic evolution of the Arctic margins and trans-Arctic links with adjacent orogens. *Edited by* Piepjohn, Strauss, Reinhard and McClelland Geological Society of America Special Paper. **541**, pp. 231–254.

Mattinson, J.M. 2005. Zircon U–Pb chemical abrasion ("CA-TIMS") method: combined annealing and multi-step partial dissolution analysis for improved precision and accuracy of zircon ages. Chemical Geology, **220**: 47–66. doi:10.1016/j.chemgeo.2005.03.011.

McClelland, W.C., Strauss, J.V., Colpron, M., Gilotti, J.A., Faehnrich, K., Malone, S.J., et al. 2021. 'Taters versus sliders: evidence for a long-lived history of strike-slip displacement along the Canadian Arctic transform system (CATS). GSA Today, **31**: 4–11. doi:10.1130/GSATG500A.1.

McClelland, W.C., Strauss, J.V., Gilotti, J.A., and Colpron, M. 2022. Paleozoic evolution of the northern Laurentian margin: evaluating links between Caledonian, Ellesmerian and Cordilleran Orogens. *In* Laurentia: an evolving continent. *Edited by* Whitmeyer, and Kellett, Geological Society of America Memoir 220, In press.

Mitjavila, J., Marti, J., and Soriano, C. 1997. Magmatic evolution and tectonic setting of the Iberian pyrite belt volcanism. Journal of Petrology, **38**(6): 727–755. doi:10.1093/petroj/38.6.727.

Murchison, R.I. 1839. The Silurian system. John Murray, London.

Nowlan, G.S. 2019. Report on twenty-one samples from the Peel Canyon section (collectors Tyler Allen and Tiffani Fraser) and the Nadaleen Mountain section (collector Justin Strauss), Yukon; Fire Bay, Ellesmere Island, Nunavut (collector Justin Strauss) and samples from the Day and Megunticook formations, Maine, U.S.A. Submitted by Justin Strauss (Dartmouth College) for conodont analysis. NTS 106C/06, 106E/l3, 560D/08. Geological Survey of Canada, Paleontological Report 001-GSN-2019. Ottawa. 9p.

Pearce, J.A. 1982. Trace element characteristics of lavas from destructive plate boundaries. Andesites, **8**: 525–548.

Pearce, J.A. 1996. A user's guide to basalt discrimination diagrams. Geological Association of Canada Short Course Notes 12. St. John's, NL, pp. 79–113.

Pearce, J.A. 2008. Geochemical fingerprinting of oceanic basalts with applications to ophiolite classification and the search for archean oceanic crust. Lithos, **100**(1–4): 14–48. doi:10.1016/j.lithos.2007.06.016.

Pearce, J.A., and Norry, M.J. 1979. Petrogenetic implications of Ti, Zr, Y, and Nb variations in volcanic rocks. Contributions to Mineralogy and Petrology, **69**(1): 33–47. doi:10.1007/BF00375192.

Pearce, J.A., Harris, N.B., and Tindle, A.G. 1984. Trace element discrimination diagrams for the tectonic interpretation of granitic rocks. Journal of Petrology, **25**(4): 956–983. doi:10.1093/petrology/25.4.956.

Pearce, J.A., Stern, R.J., Bloomer, S.H., and Fryer, P. 2005. Geochemical mapping of the Mariana arc-basin system: implications for the nature and distribution of subduction components. Geochemistry, Geophysics, Geosystems, **6**(7): Q07006. doi:10.1029/2004GC000895.

Pecha, M.E., Gehrels, G.E., McClelland, W.C., Giesler, D., White, C., and Yokelson, I. 2016. Detrital zircon U-Pb geochronology and Hf isotope geochemistry of the Yukon-Tanana terrane, Coast Mountains, southeast Alaska. Geosphere, **12**: 1556–1574. doi:10.1130/GES01303.1.

Perner, J. 1899. Etudes sur les graptolites de Bohême, III. Monographie des graptolites de l'Etage E, section b. Raimund Gerhard, Prague. pp. 1–24

Piepjohn, K., von Gosen, W., and Tessensohn, F. 2016. The Eurekan deformation in the arctic: an outline. Journal of the Geological Society, **173**: 1007–1024. doi:10.1144/jgs2016-081.

Piepjohn, K., von Gosen, W., Läufer, A., McClelland, W.C., and Estrada, S. 2013. Ellesmerian and Eurekan fault tectonics at the northern margin of Ellesmere Island (Canadian High Arctic). Journal of the German Society for Geosciences, **164**: 81–105.

Piercey, S.J., Mortensen, J.K., Murphy, D.C., Paradis, S., and Creaser, R.A. 2002. Geochemistry and tectonic significance of alkalic mafic magmatism in the Yukon-Tanana terrane, Finlayson Lake region, Yukon. Canadian Journal of Earth Sciences, **39**(12): 1729–1744. doi:10.1139/e02-090.

Rollinson, H. 1993. Using geochemical data. Routledge,London. doi:10.4324/9781315845548.

Saccani, E. 2015. A new method of discriminating different types of post-Archean ophiolitic basalts and their tectonic significance using Th-Nb and Ce-Dy-Yb systematics. Geoscience Fronteirs, **6**: 481–501. doi:10.1016/j.gsf.2014.03.006.

Saunders, A.D., and Tarney, J. 1984. Geochemical characteristics of basaltic volcanism within back-arc basins. Geological Society, London, Special Publications, **16**(1): 59–76. doi:10.1144/GSL.SP.1984.016.01.05.

Saylor, J.E., and Sundell, K.E. 2016. Quantifying comparison of large detrital geochronology data sets. Geosphere, **12**: 203–220. doi:10.1130/GES01237.1.

Saylor, J.E., Jordan, J.C., Sundell, K.C., Wang, X., Wang, S., and Deng, T. 2017. Topographic growth of the Jishi Shan and its impact on basin and hydrology evolution, NE Tibetan Plateau. Basin Research, **30**: 544–563. doi:10.1111/bre.12264.

Shervais, J.W. 1982. Ti-V plots and the petrogenesis of modern and ophiolitic lavas. Earth and Planetary Science Letters, **59**(1): 101–118. doi:10.1016/0012-821X(82)90120-0.

Shervais, J.W. 2022. The petrogenesis of modern and ophiolitic lavas reconsidered: Ti-V and Nb-Th. Geoscience Frontiers, **13**(2): 101319. doi:10.1016/j.gsf.2021.101319.

Strauss, J.V., Hoiland, C.W., Ward, W., Johnson, B.G., Nelson, L., and McClelland, W.C. 2017. Orogen transplant: taconic–caledonian magmatism in the Brooks range of Alaska. Geological Society of America Bulletin, **129**: 649–676. doi:10.1130/B31593.1.

Strauss, J.V., Macdonald, F.A., Taylor, J.F., Repetski, J.E., and McClelland, W.C. 2013. Laurentian origin for the north slope of Alaska: implications for the tectonic evolution of the Arctic. Lithosphere, **5**: 477–482. doi:10.1130/L284.1.

Sun, S.S., and McDonough, W.F. 1989. Chemical and isotopic systematics of oceanic basalts: implications for mantle composition and processes. Geological Society, Special Publications, London. vol. **42**, pp. 313–345.

Taylor, B., and Martinez, F. 2003. Back-arc basin basalt systematics. Earth and Planetary Science Letters, **210**(3–4): 481–497. doi:10.1016/S0012-821X(03)00167-5.

Taylor, S.R., and McLennan, S.M. 1995. The geochemical evolution of the continental crust. Reviews of Geophysics, **33**(2): 241–265. doi:10.1029/95RG00262.

Trettin, H.P. 1969. Pre-Mississippian geology of northern Axel Heiberg and northwestern Ellesmere Islands, Arctic archipelago. Geological Survey of Canada Bulletin, **171**: 82.

Trettin, H.P. 1987. Pearya: a composite terrane with Caledonian affinities in northern Ellesmere Island. Canadian Journal of Earth Sciences, **24**: 224–245. doi:10.1139/e87-025.

Trettin, H.P. 1994. Pre-carboniferous geology of the northern part of the Arctic Islands: Hazen fold belt and adjacent parts of the central Ellesmere fold belt, Ellesmere Island. Geological Survey of Canada Bulletin, **430**: 248.

Trettin, H.P. 1996. Geology, parts of Cape Stallworthy and Bukken Fiord, district of Franklin, Northwest Territories. Geological Survey of Canada, Map 1884A, scale 1:250 000.

Trettin, H.P. 1998. Pre-carboniferous geology of the northern part of the Arctic Islands: northern Heiberg fold belt, Clements Markham fold belt, and Pearya. Geological Survey of Canada Bulletin, **425**: 401.

Trettin, H.P., and Mayr, U. 1996. Geology, part of Otto Fiord, district of Franklin, Northwest Territories. Geological Survey of Canada, Map 1885A, scale 1:250 000.

Trettin, H.P., and Nowlan, G.S. 1990. Middle ordovician sedimentary and volcanic rocks at Fire Bay, Emma Fiord, northwestern Ellesmere Island. Geological Survey of Canada Paper, **90-1D**, pp. 147–151.

Trettin, H.P., Parrish, R., and Loveridge, W.D. 1987. U-Pb age determinations of Proterozoic to Devonian rocks from northern Ellesmere Island, Arctic Canada. Canadian Journal of Earth Sciences, **24**: 246–256. doi:10.1139/e87-026.

Vaughan, A.P., and Scarrow, J.H. 2003. K-rich mantle metasomatism control of localization and initiation of lithospheric strike-slip faulting. Terra Nova, **15**(3): 163–169. doi:10.1046/j.1365-3121.2003.00485.x.

Vermeesch, P. 2018*a*. Dissimilarity measures in detrital geochronology. Earth Science Reviews **178**: 310–321. doi:10.1016/j.earscirev.2017.11.027.

Vermeesch, P. 2018*b*. IsoplotR: a free and open toolbox for geochronology. Geoscience Frontiers, **9**: 1479–1493. doi:10.1016/j.gsf.2018.04.001.

Vermeesch, P. 2021. Maximum depositional age estimation revisited. Geoscience Frontiers, **12**: 843–850. doi:10.1016/j.gsf.2020.08.008.

Vervoort, J.D., and Blichert-Toft, J. 1999. Evolution of the depleted mantle: Hf isotope evidence from juvenile rocks through time. Geochimica et Cosmochimica Acta, **63**: 533–556. doi:10.1016/S0016-7037(98)00274-9.

Walker, J.D., Geisman, J.W., Bowring, S.A., and Babcock, L.E. 2018. Geologic time scale v. 5.0. Geological Society of America. doi:10.1130/2018.CTS005R3C.

White, C., Gehrels, G.E., Pecha, M., Giesler, D., Yokelson, I., and McClelland, W.C. 2016. U-Pb and Hf isotope analysis of detrital zircons from Paleozoic strata of the southern Alexander terrane (southeast Alaska). Lithosphere, **8**: 83–96. doi:10.1130/L475.1.

Winchester, J.A., and Floyd, P.A. 1977. Geochemical discrimination of different magma series and their differentiation products using immobile elements. Chemical Geology, **20**: 325–343. doi:10.1016/0009-2541(77)90057-2.